Contrasting Mechanisms of Aromatic and Aryl-Methyl Substituent Hydroxylation by the Rieske Monooxygenase Salicylate 5-Hydroxylase

Melanie S. Rogers,[†] Adrian M. Gordon,[‡] Todd M. Rappe,[§]
Jason D. Goodpaster,[‡] and John D. Lipscomb*[†]

[†]Department of Biochemistry, Molecular Biology, and Biophysics and Center for Metals in Biocatalysis, University of Minnesota, Minneapolis, Minnesota 55455, United States

[‡]Department of Chemistry, University of Minnesota, Minneapolis, Minnesota 55455, United States.

[§]Minnesota NMR Center, University of Minnesota, Minneapolis, Minnesota 55455, United States.

*Address correspondence to:

John D. Lipscomb
University of Minnesota
Department of Biochemistry, Biophysics and Molecular Biology
6-155 Jackson Hall
321, Church Street S.E.
Minneapolis, Minnesota, 55455, USA.
E-mail: lipsc001@umn.edu

ABSTRACT: The hydroxylase component (S5HH) of salicylate-5-hydroxylase catalyzes C5 ring hydroxylation of salicylate but switches to methyl hydroxylation when a C5 methyl substituent is present. Use of $^{18}O_2$ reveals that both aromatic and aryl-methyl hydroxylations result from monooxygenase chemistry. The functional unit of S5HH comprises a nonheme Fe(II) site located 12 Å across a subunit boundary from a one-electron reduced Rieske-type iron-sulfur cluster. Past studies determined that substrates bind near the Fe(II), followed by O_2 binding to the iron to initiate catalysis. Stopped-flow-single-turnover reactions (STO) demonstrated that the Rieske cluster transfers an electron to the iron site during catalysis. It is shown here that fluorine ring substituents decrease the rate constant for Rieske electron transfer, implying a prior reaction of an Fe(III)-superoxo intermediate with substrate. We propose that the iron becomes fully oxidized in the resulting Fe(III)-peroxo-substrate-radical intermediate, allowing Rieske electron transfer to occur. STO using 5-CD_3-salicylate-d_8 occurs with an inverse KIE. In contrast, STO of a 1:1 mixture of unlabeled and 5-CD_3-salicylate-d_8 yields a normal product isotope effect. It is proposed that aromatic and aryl-methyl hydroxylation reactions both begin with Fe(III)-superoxo reaction with a ring carbon, yielding the inverse KIE due to $sp^2 \rightarrow sp^3$ carbon hybridization. After Rieske electron transfer, the resulting Fe(III)-peroxo-salicylate intermediate can continue to aromatic hydroxylation, whereas the equivalent aryl-methyl intermediate formation must be reversible to allow the substrate exchange necessary to yield a normal product isotope effect. The resulting Fe(III)-(hydro)peroxo intermediate may be reactive or evolve through a high-valent iron intermediate to complete the aryl-methyl hydroxylation.

INTRODUCTION

Rieske oxygenases (ROs) are nonheme iron-containing enzymes that catalyze a remarkably expansive range of reactions and act upon a diverse group of substrate chemical types.[1-10] Found widely across Nature,[11-29] the ROs are increasingly appreciated for their roles and applications in human health,[28, 30-33] environmental biotechnology,[34-41] agriculture,[42] and chemoenzymatic synthesis.[43-48] Collectively, the catalytic repertoire of the RO family exceeds even those of other well-studied oxygenases, including cytochrome P450, dinuclear iron-containing hydrocarbon monooxygenases, flavin oxygenases, and α-ketoacid-linked monooxygenases.[7, 49-55]

The RO family has a highly conserved quaternary structure (generally $\alpha_3\beta_3$ or α_3) with a Rieske-type [2Fe-2S] iron-sulfur cluster and a 2-His-1-carboxylate type mononuclear Fe(II) site in each α-subunit. The head-to-tail organization of the α-subunits places the Rieske cluster of one subunit adjacent to the mononuclear iron site of another, and this cross-subunit boundary pair of metal centers is considered to be the reactive unit.[56] Oxygen activation and substrate oxidation occur at the mononuclear iron site with the reduced Rieske cluster [Fe(II)-Fe(III)] providing an essential electron for the process.[57-59] Despite the many fundamental similarities of the RO enzymes, considerable specificity in substrate selection, reaction type, and regiospecificity is observed for individual family members. X-ray crystal structures of ROs that catalyze a range of reaction types fail to distinguish a basis for this specificity in the structural regions encompassing the Rieske cluster, the residues between the metal centers, and mononuclear iron ligation, which are remarkably conserved.[31, 38, 39, 56, 59-73] Progress has been made in understanding the key features of the active site surrounding the mononuclear iron that orient the substrate and provide a level of regiospecificity.[27, 59, 72, 74-77] However, there is currently little insight into whether the various reactivities require different types of activated oxygen species or how such divergent species might evolve from a highly conserved metal center.

The aromatic cis-dihydrodiol-forming subclass of Rieske dioxygenases have been the most intensively studied in terms of delineating the substrate range, mechanism, and biophysical properties.[49, 58, 76, 78-86] Transient kinetic and computational studies coupled with diagnostic substrates and spectroscopic techniques have led to the proposal that substrate binding near the mononuclear Fe(II) site causes loss of a water ligand, permitting subsequent O_2 binding to the

metal to yield an Fe(III)-superoxo intermediate (Scheme 1).[82, 84, 87] This intermediate is proposed to react at an electron rich carbon of the aromatic substrate ring based on two key observations: (i) the rate constant for electron transfer from the Rieske cluster was shown to depend on the specific substrate present in the active site, implying reaction of the one electron reduced oxygen species with substrate before transfer of the second electron required for product formation,[78, 84] and (ii) using a set of ring fluorinated substrate analogs, the log of the rate constant for Rieske electron transfer was shown to correlate linearly with the net charge at the position of attack for cis-dihydroxylation in benzoate 1,2 dioxygenase (BZDO).[84] During reaction with the Fe(III)-superoxo intermediate, one-electron oxidation of the aromatic ring would yield an Fe(III)-peroxo-aryl radical intermediate. The now fully oxidized mononuclear Fe(III) site would allow electron transfer from the reduced Rieske cluster to yield a bridging Fe(III)-aryl-peroxo intermediate that can undergo O-O bond cleavage to yield an epoxide intermediate by a mechanism akin to one proposed for electrophilic aromatic substitution.[88-91] The cis-dihydrodiol product could be formed by reaction of the Fe(III)-OH with the carbocation that results from ring-opening of the epoxide.[82] Several other mechanistic proposals have been advanced[7] based on formation of a dioxetane,[56, 92, 93] hydroperoxo,[81, 94] or HO-Fe(V)=O intermediates.[58, 86, 95] However, formation of these initially reactive species requires transfer of the Rieske electron prior to reaction of the activated oxygen species with the substrate. The strong dependence of the rate constant for electron transfer from the Rieske cluster on the type and charge distribution of the substrate suggests that electron transfer before a reaction with the substrate is unlikely.[84]

Scheme 1. Mechanism Proposed for Rieske Dioxygenases

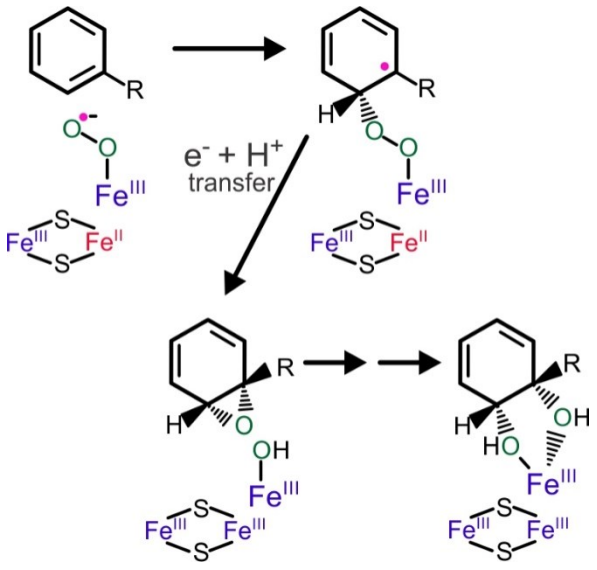

More recently, attention has turned to the Rieske monooxygenase class, members of which fall into several subclasses that catalyze hydroxylation of aromatic,[68, 96, 97] cyclic,[26, 70] and aliphatic[12, 19, 98, 99] substrates. Additionally, hydroxylation of heteroatoms,[100] dehydrogenation,[101] desaturation, [21] and O- and N- demethylation[42, 71, 73, 102-105] of numerous environmentally relevant or economically valuable substrates have been reported.[5, 106, 107] Our studies have focused on salicylate 5-hydroxylase (S5H) which catalyzes the formation of gentisate (2,5-dihydroxybenzoate) as part of one of the naphthalene biodegradation pathways in *Ralstonia*.[108, 109] The hydroxylase component (S5HH) of the three component S5H system (reductase, ferredoxin, and hydroxylase) appears to catalyze strictly monooxygenase chemistry, while conserving both the $\alpha_3\beta_3$ quaternary structure and metal cofactors of Rieske dioxygenases.[59, 108-110] The initial studies of the S5HH mechanism surprisingly showed that the rate constant for electron transfer from the Rieske cluster when benzoate was used as the substrate in place of salicylate was slowed approximately 20-fold. Thus, the reaction exhibited the same dependence on the specific structure and electronic characteristics of the substrate as described for the Rieske dioxygenases.[84, 108] A very similar mechanism was proposed based on initial attack by an Fe(III)-superoxo species (Scheme 2). The two mechanisms were proposed to differ in either the mechanism of O-O bond cleavage or, if an epoxide is formed in both cases, the steps subsequent to its opening. The monooxygenase reaction would involve internal hydride transfer rather than hydroxyl transfer from Fe(III)-OH. Ligand-to-metal charge transfer from the aromatic phenolate product from salicylate during the S5HH catalyzed reaction allowed direct demonstration of the formation of a chromophoric Fe(III)-product complex as the penultimate step in the reaction cycle.

Scheme 2. Mechanism Proposed for Rieske Monooxygenase S5HH

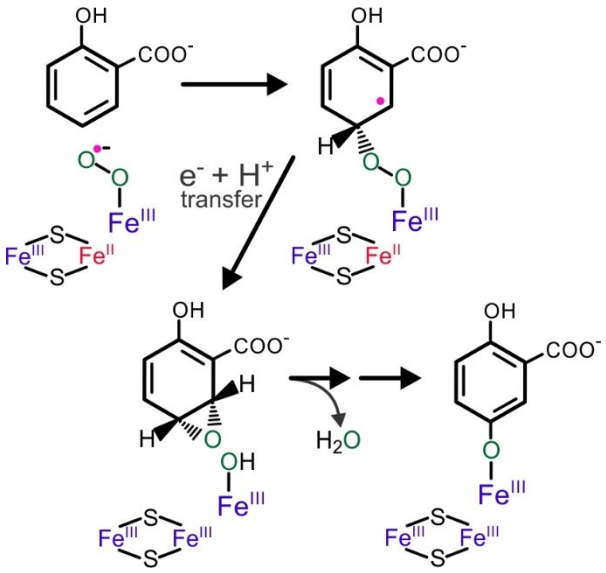

S5HH is a particularly relevant target for detailed mechanistic studies, because: (i) it has been structurally characterized,[59] (ii) it reacts with a wide variety of potentially diagnostic salicylate analogs including benzoate, the substrate of cis-diol-forming BZDO,[108, 109, 111] and (iii) it reportedly catalyzes aryl-methyl substituent hydroxylation in addition to aromatic hydroxylation.[109] The latter two reactions are mechanistically distinct where encountered in other well-studied types of oxygenases,[112-114] and thus they offer the opportunity to explore catalytic diversity in a single, native active site of a RO. In the current study, the reactivity and the mechanism of O_2 activation by S5HH are explored in more detail using alternative substrates, product identification, computational approaches, and kinetic and product isotope effects. The results support a common mechanism for all RO reaction types through the point of electron transfer from the Rieske cluster. Thereafter, the pathways appear to diverge in response to the electronic properties and positioning of the substrate in the active site as manifested in the kinetics of subsequent reaction steps.

■ EXPERIMENTAL PROCEDURES

General Methods. Standard procedures and chemical suppliers are described in the Supporting Information.

Production of S5H Proteins. S5H reductase (S5HR), S5H ferredoxin (S5HF), and His-tagged S5HH were purified as previously described.[108] His-tagged S5HH destined for tag cleavage was purified as previously described for His-tagged S5HH up to the enzyme bound column wash step.[108] At this point, the column (25 ml Roche cOmplete His-Tag purification column) was washed with 50 mM HEPES, 300 mM NaCl, 10 % glycerol, 20 mM imidazole, pH 8 buffer without dithiothreitol (wash buffer). Thrombin cleavage of the His-tag was based on the method of Hefti.[115] Thrombin (1000 U, Sigma-Aldrich) was dissolved in 20 ml wash buffer and applied to the column. The thrombin-containing buffer was recirculated overnight using a peristaltic pump. The cleaved protein was eluted with wash buffer and concentrated. The concentrated protein was applied to a Sephacryl-300 HR column (2.5 x 120 cm) equilibrated in 50 mM HEPES, 200 mM NaCl, pH 8 for final purification and buffer exchange. Fractions containing S5HH were pooled, concentrated, and glycerol was added to 5 %. The enzyme was flash-frozen in liquid nitrogen and stored at -80 °C. Reduced S5HH used for single turnover experiments was prepared as described.[108]

Preparation of Substrates and Oxygen-containing Solutions. Substrate solutions were prepared in 50 mM HEPES, 100 mM NaCl, 5 % glycerol, pH 8 buffer (standard buffer). Substrates with low aqueous solubility were prepared at high concentration in methanol and then diluted into the standard buffer to give a final methanol concentration of < 2 %. Oxygen-saturated solutions (1.8 mM) were prepared by bubbling O_2 gas through buffer solutions in capped Wheaton serum vials with needle venting at 4 °C. $^{18}O_2$ solutions were prepared by preparing a capped Wheaton serum vial completely filled with anaerobic standard buffer (14 ml). Then $^{18}O_2$ gas was flowed into the inverted vial equipped with a vent needle to allow 2 ml of buffer to be displaced . The resulting solution was vortexed, and then vigorously stirred on ice for 30 m (1.8 mM $^{18}O_2$ at 4 °C).

Stopped-flow Measurements and Analysis of Single Turnover Reactions. The pre-steady state kinetics of reduced S5HH with substrates were measured and the time courses fit using nonlinear regression analysis to a multi-summed-exponential expression as previously described.[108] All enzyme concentrations in this study refer to active site concentrations rather than total protein concentration in the trimeric enzyme. Standard reaction conditions after mixing: 30 μM reduced S5HH active sites (His-tag removed), 5 mM substrate, 900 μM O_2, standard buffer, 4 °C.

Kinetic Isotope Effects. The kinetic isotope effect (KIE) for the Rieske oxidation reaction was measured for salicylate and 5-CH_3-salicylate via stopped-flow single turnover experiments. Substrate solutions (10 mM) were prepared and then the UV-visible spectrum of each solution was measured. Appropriate dilutions were made so that the solutions gave the same absorbance at λ_{max}. Reduced S5HH (30 μM) was reacted with salicylate, salicylate-d_6, 5-methyl-salicylate or 5-methyl-salicylate-d_8 (5 mM) in oxygen-saturated (900 μM) standard buffer using an Applied Photophysics SX.18MV stopped-flow spectrophotometer at 4 °C and monitored at 453 nm (all concentrations after mixing). The KIE was determined from the ratio of the Rieske oxidation first phase reciprocal relaxation times ($1/\tau_1$) for unlabeled substrate and fully deuterated substrate.

Rapid Chemical Quench. Anaerobic procedures were performed in a Coy anaerobic chamber. Deoxygenated, stoichiometrically reduced, His-tagged S5HH (230 μM active sites) plus the internal standard (ISTD) 3,5-dihydroxy-benzoic acid (30 μM) was reacted with 5-methyl-salicylate (5 mM) in O_2 saturated standard buffer (900 μM O_2) using an Update Instruments 715 rapid mixing ram syringe system (all concentrations after mixing). Control experiments showed that the ISTD is not an S5HH substrate or inhibitor. The single turnover reaction with 5-methyl-salicylate was chemically quenched at discrete timepoints by rapid dispensation into an equal volume of rapidly stirring 10 % trifluoroacetic acid (TFA) in a Reacti-vial. After vortexing for 30 s, an equal volume of 1 M HEPES, pH 8 was added. The sample was centrifuged to remove precipitated protein. Product formation at each quench time point was analyzed using high-pressure liquid chromatography (HPLC) (See Supporting Information).

Reactions with $^{18}O_2$ and $H_2{}^{18}O$. Incorporation of oxygen from O_2 into salicylate substrates was assessed via single turnover reactions of stoichiometrically reduced S5HH (25 μM) with salicylate (5.37 mM), 4-fluoro-salicylate (56.7 mM), 5-fluoro-salicylate (56.6 mM), or 5-methyl-salicylate (5.66 mM) in the presence of $^{18}O_2$ (1.55 mM) at 23 °C. Anaerobic substrate solutions were added to reduced S5HH prior to addition of $^{18}O_2$ saturated buffer (total volume was 2.32 ml). After 1 h, the reactions were processed as described in Supporting Information for analysis using gas-chromatography-mass spectrometry (GCMS).

The ^{18}O-buffer was prepared by lyophilizing standard buffer, and then adding $H_2{}^{18}O$ to the initial buffer volume. For single turnover reactions in $H_2{}^{18}O$, S5HH was exchanged into ^{18}O-buffer via concentration and dilution (yielding 96 % $H_2{}^{18}O$). To ensure full exchange of S5HH

active site water molecules, the enzyme was incubated in ^{18}O-buffer overnight at room temperature. S5HH was deoxygenated on ice by flowing high-purity argon gas over the surface with stirring and then stoichiometrically reduced with sodium dithionite in a Coy anaerobic chamber. The enzyme (280 μM) was reacted with salicylate (13.5 mM) or 5-methyl-salicylate (13.9 mM) as described above for the $^{18}O_2$ incorporation reaction except that unlabeled oxygen gas was utilized (total solution volume 0.49 ml). The reactions were then processed for GCMS analysis as described in Supporting Information.

Product Isotope Effect. Single turnover reactions of stoichiometrically reduced S5HH (28 μM) with a solution of salicylate (7.46 mM) and salicylate-d_6 (7.24 mM) or a solution of 5-methyl-salicylate (7.33 mM) and 5-methyl-salicylate-d_8 (7.5 mM) in oxygen-saturated (1.55 mM after component additions) standard buffer at 23 °C were conducted. After 1 h, the reactions were processed for GCMS analysis as described in Supporting Information. Protiated and deuterated products were determined from the mass spectra of undiluted samples and protiated and deuterated substrates were determined from the mass spectra of the samples diluted 200-fold with dichloromethane. The product isotope effect was computed after corrections for the small differences in substrate concentrations as described in Supporting Information.

Product Identification by NMR Spectroscopy. Steady-state reactions were conducted to accumulate sufficient quantities of S5HH reaction products for NMR spectroscopy. The reactions contained NADH (5 mM), S5HR (0.4 μM), S5HF (3.2 μM), S5HH (14 μM), and substrate (4.2 mM) in O_2-saturated (1.55 mM after component additions) standard buffer (5.9 ml, 23 °C). Substrates analyzed were: 4-fluoro-salicylate, 5-fluoro-salicylate, 5-methyl-salicylate, or 3-methyl-benzoate. Reactions were conducted in a Reacti-vial with stirring.

S5HH reactions were quenched with the addition of an equal volume of trifluoroacetic acid (10 %) while stirring. The solution was vortexed and then centrifuged. An equal volume of 1 M HEPES, pH 8.0 was added to the supernatant containing the reaction product. The reaction product was purified via HPLC using multiple separate 1 ml injections (see Supporting Information).[108] Fractions were collected and assessed via UV-visible spectroscopy. Fractions corresponding to the elution time of the product chromatogram peak (detected at 238 nm) were pooled and lyophilized. The lyophilized product was dissolved in CD_3OD prior to NMR spectroscopy.

^{1}H NMR data for the purified S5HH reaction product with substrates 5-methyl-salicylate or 3-methyl-benzoate were collected at the UMN Chemistry NMR Center using a Bruker Avance III HD Nanobay AX-400. Spectra of authentic 5-hydroxymethyl-salicylate and 3-hydroxymethyl-benzoate standards were also recorded.

NMR data for the purified S5HH reaction product with substrates 4-fluoro-salicylate and 5-fluoro-salicylate were collected at the Minnesota NMR Center using a 600-MHz Bruker Avance NEO spectrometer with a 5-mm CPTCI ^{1}H(^{19}F)/^{13}C/^{15}N/^{2}H Z-gradient cryoprobe controlled by Topspin 4.0 software. Spectra were acquired at 25 °C in CD_3OD and referenced through the solvent lock (^{2}H) signal according to the IUPAC recommendations for secondary referencing and to the manufacturer's protocols.

Product Identification by HPLC. 5-Hydroxymethyl-salicylate and 3-hydroxymethyl-benzoate produced from steady state reactions of S5HH with 5-methyl-salicylate or 3-methyl-benzoate, respectively, under the conditions described above were identified by comparison of their HPLC retention time to those of authentic product standards. HPLC was performed as previously described.[108]

Computational Methods. All calculations were performed using the M06-2X functional[116] and the 6-311+(2df,p) basis set[117] within the electronic structure modeling program Gaussian 16 version c01.[118] Geometries were optimized for salicylates and benzoates in their deprotonated conjugate base forms. The SMD (solvation model based on density) continuum solvation model using a dielectric constant of 5.6968, appropriate for the hydrophobic enzyme active site, was used.[119] CM5 (charge model 5) atomic charges were calculated with charges of hydrogens summed into those of heavy atoms.[120] Vibrational frequency calculations were performed for each optimized structure and thermal and entropic contributions added to the self-consistent field energy. Bond dissociation free energies were calculated for bonds broken and formed in the enzyme catalyzed hydroxylation of the substrate.

Bond dissociation free energy (BDFE) of the bond R-X was calculated using Equation 1 where R-X represents the salicylate or benzoate molecule, R• represents the molecule after bond dissociation, and X• represents the dissociated atom (either H or F).

$$BDFE(R\text{-}X) = \Delta G(R\bullet) + \Delta G(X\bullet) - \Delta G(R\text{-}X) \qquad \text{Equation 1}$$

Here, we only report calculations using the M06-2X functional; however, additional computations were also performed using the ωB97XD functional,[121] and these computations showed that identical conclusions would be reached.

Electrostatic potential surface maps were produced on the ρ = 0.02 au contour of the molecular electronic density, from the optimized structures computed with the parameters described in the Computational Methods section of Experimental Procedures. Electrostatic potential surface map images were made in GaussView 6.1.[122]

■ RESULTS

S5HH Reactions with Substituted Salicylates and Benzoates. Early studies used whole cell biotransformations or cell-free extracts to investigate the substrate range of S5HH.[109, 110] Later, these studies were extended to the use of purified enzyme without direct product identification.[111] In the current study, we use purified enzyme together with product characterization and various single and multiple turnover kinetic techniques to examine the mechanism(s) of O_2 activation and substrate oxygenation by this Rieske monooxygenase. The gentisate product of the reaction of S5HH with salicylate has been previously identified [108, 110] The products from reactions of purified S5HH with fluorine- and methyl-substituted salicylates and benzoates are reported in Table 1 and the methods used for product identification are detailed in Experimental Procedures and Supporting Information Figures S1-S13.

Table 1. Summary of Reactions of Fluoro- and Methyl- Substituted Salicylates and Benzoates with Purified S5HH

Substrate	Product	Rieske oxidation kinetics[a] $1/\tau_1$ (s^{-1})	Abs_{700} increase kinetics[b] $1/\tau$ (s^{-1})	Relative ΔAbs_{700} in first phase[c]	Computed Substrate Atomic Charge		
					C4	C5	C6
None	None	0.14 ± 0.01	0.18 ± 0.01	0.05	-	-	-
Salicylate (Sal)	5-OH-Sal[d,e]	119 ± 10	23.0 ± 1.9	1.0	-0.0169	-0.0451	-0.0217
3-F-Sal	3-F,5-OH-Sal[f]	36.7 ± 2.6	7.9 ± 0.6	0.99	-0.0052	-0.0269	-0.0234
4-F-Sal	4-F,5-OH-Sal[g,h]	1.18 ± 0.09	1.3 ± 0.1	0.83	+0.0823	-0.0310	+0.0016
5-F-Sal	5-F,6-OH-Sal[g,h]	55.9 ± 3.9	4.8 ± 0.4	0.22	-0.0136	+0.0700	-0.0041
6-F-Sal	5-OH,6-F-Sal[f]	26.4 ± 2	13.6 ± 1	0.99	-0.0088	-0.0313	+0.0882
Benzoate (Ben)	3-OH-Ben[d]	3.9 ± 0.3	2.3 ± 0.2	0.91	-0.0222	-0.0227	-0.0216
2-F-Ben	2-F,5-OH-Ben[f]	2.5 ± 0.2	2.2 ± 0.2	0.65	-0.0043	-0.0245	-0.0098
3-CH_3-Ben	3-CH_2OH-Ben[g,h,i]	0.24 ± 0.05	0.21 ± 0.05	0.06	-0.0281	-0.0303	-0.0242
5-CH_3-Sal	5-CH_2OH-Sal[g,h,i,j]	3.3 ± 0.3	1.43 ± 0.1	0.07	-0.0317	-0.0436	-0.0163
5-CF_3-Sal	None detected	0.42 ± 0.05	0.51 ± 0.05	0.05	+0.0102	-0.0648	+0.0091

[a]Reaction conditions: 30 μM reduced S5HH (without His-tag), 5 mM substrate, 900 μM O_2, 50 mM HEPES, 100 mM NaCl, 5 % glycerol, pH 8, 4 °C. The reaction time courses are best fit with a 3-summed exponential time course. The fastest and largest amplitude phase ($1/\tau_1$) has been shown to correlate with product formation.[108]

[b]The absorbance at 700 nm (Abs_{700}) has been shown to arise from both a small increase due to Rieske cluster oxidation and, in some cases, a larger increase from formation of a ferric-phenolate product complex that subsequently dissociates to release the hydroxylated product and complete the catalytic cycle.[108]

[c]The largest absorbance increase at 700 nm appears to occurs when a ferric-phenolate product complex is formed and when the aromatic hydroxylation is in the salicylate C5 (or benzoate C3) position.[108]

[d]By HPLC with an authentic product standard after a single turnover and by LCMS. [108]

[e]By NMR after multiple turnover in a whole cell system.[110]

[f]Presumed product based on increase in Abs_{700} after a single turnover reaction monitored by stopped-flow spectroscopy.

[g]By NMR after steady state turnover with purified enzyme components with subsequent HPLC product purification.
[h]By GCMS of the TMS product derivative after a single turnover (4-F-salicylate reaction with $^{18}O_2$).
[i]By HPLC using an authentic product standard after steady state turnover.
[j]By NMR after multiple turnover in a whole cell system.[109]

Single Turnover Transient Kinetics of S5HH Reactions. The time course for reaction of S5HH with substrates and O_2 can be monitored by the change in Rieske cluster absorbance at 453 nm as an electron is transferred from the Rieske cluster to the mononuclear iron site (Figure 1). Past studies of the Rieske oxygenases have shown that the time course of Rieske oxidation is best fit by nonlinear regression using a 3-summed exponential equation, indicating 3 kinetic phases.[78, 84, 108, 123] The unexpected triphasic behavior for transfer of a single electron was attributed to 3 parallel reactions. This finding, along with the assumption of quasi-irreversibility of electron transfer against a substantial redox potential barrier,[124, 125] allows correlation of the reciprocal relaxation times from computed fits with rate constants for the physical reactions. Accordingly, the fastest and largest amplitude phase ($1/\tau_1$, Table 1) has been shown to correlate with the rate constant for product formation.[84, 108] The origin of the other phases remains undetermined, but they presumably result from nonproductive oxidation pathways for some of the Rieske clusters. As we have observed previously for Rieske dioxygenases,[78, 84] the Rieske oxidation kinetics of S5HH are sensitive to the chemical structure of the substrates tested here (Figure 1), indicating a direct role of the substrate in catalytic step(s) that allow the electron transfer to occur.

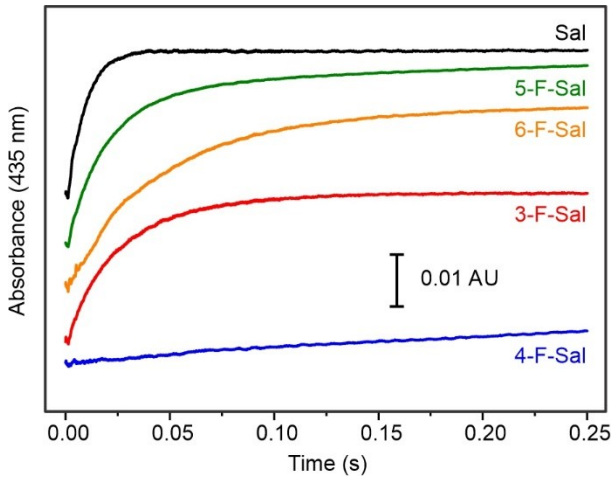

Figure 1. Single turnover time courses monitored at 453 nm for reaction of reduced S5HH (30 μM active sites) with O_2 (900 μM) and substrates (5 mM). All concentrations are after mixing. The substrates utilized are identified on the figure (abbreviations as in Table 1). The time courses are offset for clarity. Conditions: 50 mM HEPES buffer, 100 mM NaCl, 5 % glycerol, pH 8.0, 4 °C.

Fluorine substituents slow Rieske oxidation (and product formation) when placed anywhere in the ring, but in most cases, ring hydroxylation still occurs at C5 (Table 1, Figures S1-S4). An exception occurs when fluorine is placed at C5, in which case ring hydroxylation appears to occur at C6. This conclusion is supported by the direct identification of C6 hydroxylation when chlorine is placed at C5 in whole cell experiments[109] and by the NMR characterization presented here in Figures S5-S9. Also, our past studies of S5HH have shown that when products are formed with a OH at C5 (gentisate from salicylate or the equivalent 3-OH-benzoate from benzoate), a complex with a long-lived charge-transfer chromophore at ~700 nm is formed.[108] This species arises as the mononuclear Fe(III) formed during the reaction cycle shifts in the active site during the last step of the reaction to form a complex with the hydroxylated product. As shown in Figure 2, the 6-F-salicylate reaction product forms a similar intense chromophore to that seen during the reaction with salicylate, but no such chromophore is formed as 5-F-salicylate reacts. Indeed, 3- and 4-F salicylates, as well as 2-F-benzoate, form similar ~700 nm chromophores, consistent with C5 (or C3 for benzoate) hydroxylation (Table 1). The lack of a chromophore despite rapid ring hydroxylation for 5-F-salicylate is consistent with hydroxylation at a different ring position.

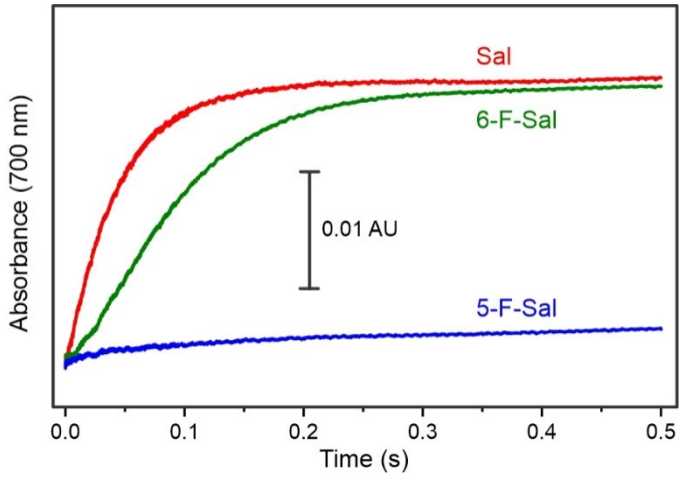

Figure 2. Single turnover time courses monitored at 700 nm for reaction of stoichiometrically reduced S5HH (30 μM) with O_2 (900 μM) and substrates (5 mM). All concentrations are after mixing. The substrates utilized are identified on the figure (See Table 1). Conditions: 50 mM HEPES buffer, 100 mM NaCl, 5 % glycerol, pH 8.0, 4 °C.

5-Methyl-Salicylate Oxygenation Occurs on Methyl Rather than the Aromatic Ring. Product identification by NMR and GCMS after either single or multiple

turnover as well as HPLC versus an authentic standard shows that 5-methyl-salicylate (5-CH_3-Sal) is oxygenated to form 5-hydroxymethyl-salicylate (5-CH_2OH-Sal, Table 1, Figures S10-S11).[109] Methyl substituent hydroxylation has also been observed in reactions of other ROs.[46, 97, 126-128] For S5HH, no evidence of ring hydroxylation was detected and no increase in absorbance at 700 nm occurred beyond that expected for oxidation of the Rieske cluster (Table 1). Each of these findings is suggestive of a distinct type of oxygenation chemistry. The single turnover reaction can again be fit by nonlinear regression using a 3-summed exponential expression indicative of 3 kinetic phases (Figure 3A). The reciprocal relaxation time for phase 1 of this reaction is decreased 35-fold from that of the salicylate reaction. Importantly, as shown in Figure 3B, the rate constant for product formation assessed by rapid chemical quench and HPLC analysis is similarly slowed (RFQ $k_1 = 4.9 \pm 1.5$ s^{-1} versus $k_1 = 4.5 \pm 0.5$ s^{-1}, rate constants increase slightly when using His-tagged S5HH).

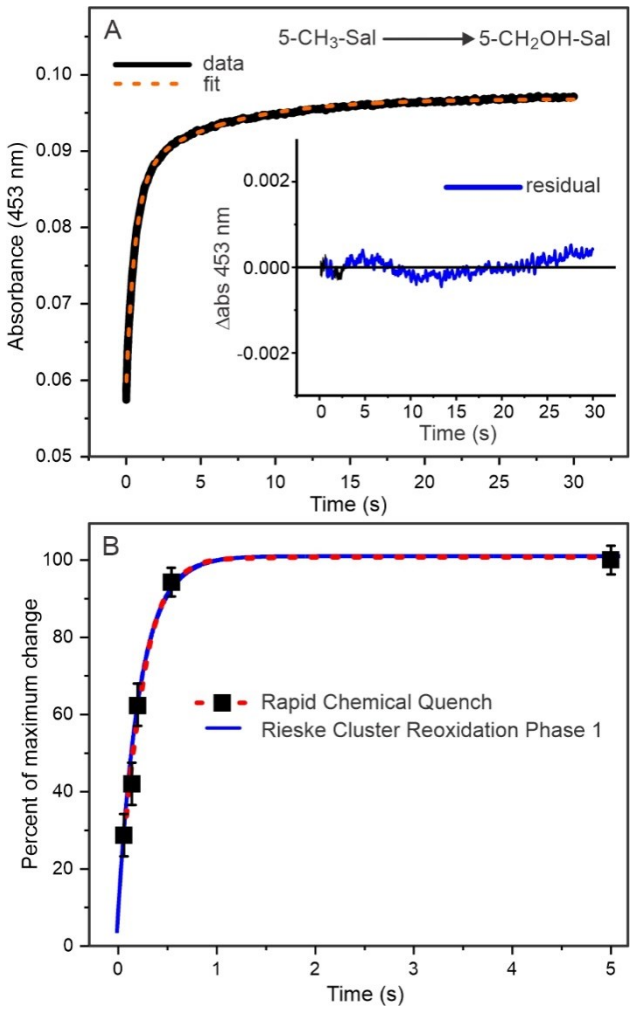

Figure 3. Time course for product formation from 5-CH_3-Sal by His-tagged S5HH. (A) Nonlinear regression 3-exponential fit (orange dashed line) is shown superimposed on the single turnover reaction time course (black). The fit residual is shown in the inset. The standard reaction conditions given in Experimental Procedures were utilized. (B) Comparison of the time course for product formation with that for phase 1 of Rieske cluster oxidation. The product formed was analyzed using RFQ and the reaction conditions are given in Experimental Procedures. HPLC analysis of the product yield from RCQ samples (■) are shown. A non-linear regression single exponential fit is superimposed on the data (red dashed line). The first phase of the single turnover time course monitored at 453 nm was extracted from the data and is shown superimposed (solid blue line).

A 5-Trifluoro-Methyl Substituent Blocks Oxygenation but not Binding. Single turnover reaction of reduced S5HH with 5-trifluoro-methyl-salicylate (5-CF_3-Sal) and O_2 was found to mimic the autooxidation of the Rieske cluster in the absence of a substrate (Figure 4). Accordingly, no product was detected from the reaction at long times (Table 1). The binding of 5-CF_3-Sal in the S5HH active site was examined by reacting S5HH with an equimolar concentration of salicylate and 5-CF_3-Sal (Figure 4, red trace). The rapid first phase of Rieske oxidation was slowed by 2.55-fold indicating that 5-CF_3-Sal binds in the active site with a similar affinity to salicylate but cannot undergo a monooxygenase reaction (Figure 4).

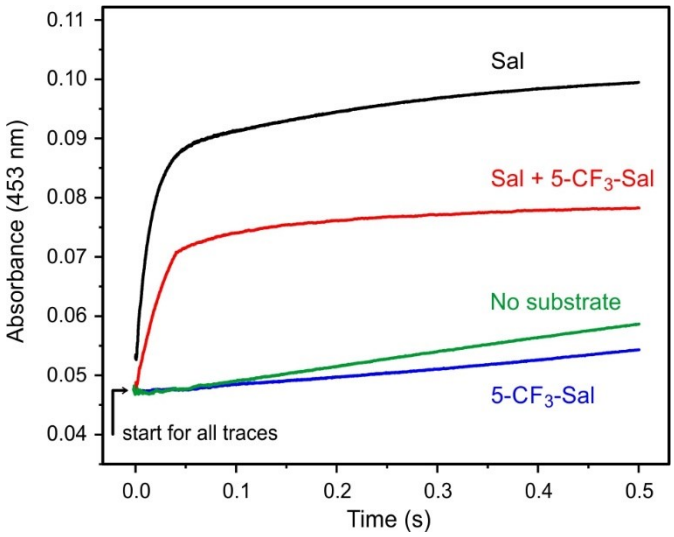

Figure 4. Stopped-flow time courses for Rieske oxidation showing the competition between salicylate and 5-CF_3-Sal for binding in the active site. Reduced S5HH (30 μM) was reacted with O_2 (900 μM) and salicylate (364 μM), 5-trifluoro-methyl-salicylate (5 mM), salicylate (364 μM) together with 5-CF_3-Sal (364 μM), or no substrate. All concentrations are after mixing. The buffer was 50 mM HEPES, 100 mM NaCl, 5 % glycerol, pH 8.0, 4 °C.

^{18}O Incorporation During S5HH Ring Hydroxylation and Aryl-Methyl Hydroxylation Reactions. Single turnover reactions of S5HH with substrates were conducted in the presence of $^{18}O_2$ to confirm that the origin of the oxygen in the product was O_2 and then to determine the percentage incorporation of ^{18}O (Figure 5 and Table 2). For both ring hydroxylation and methyl substituent hydroxylation reactions, a single ^{18}O was incorporated at >85 % occupancy, demonstrating that S5HH is a monooxygenase for both types of reaction. When the potential ^{18}O source was water, no incorporation was observed (Figure S14 and Table 2). Taken together, both data indicate that the conditions for the experiment with $^{18}O_2$ resulted in a ~15 % contamination with atmospheric O_2 rather than incorporation due to an exchange of oxygen from water into a potential reactive intermediate.

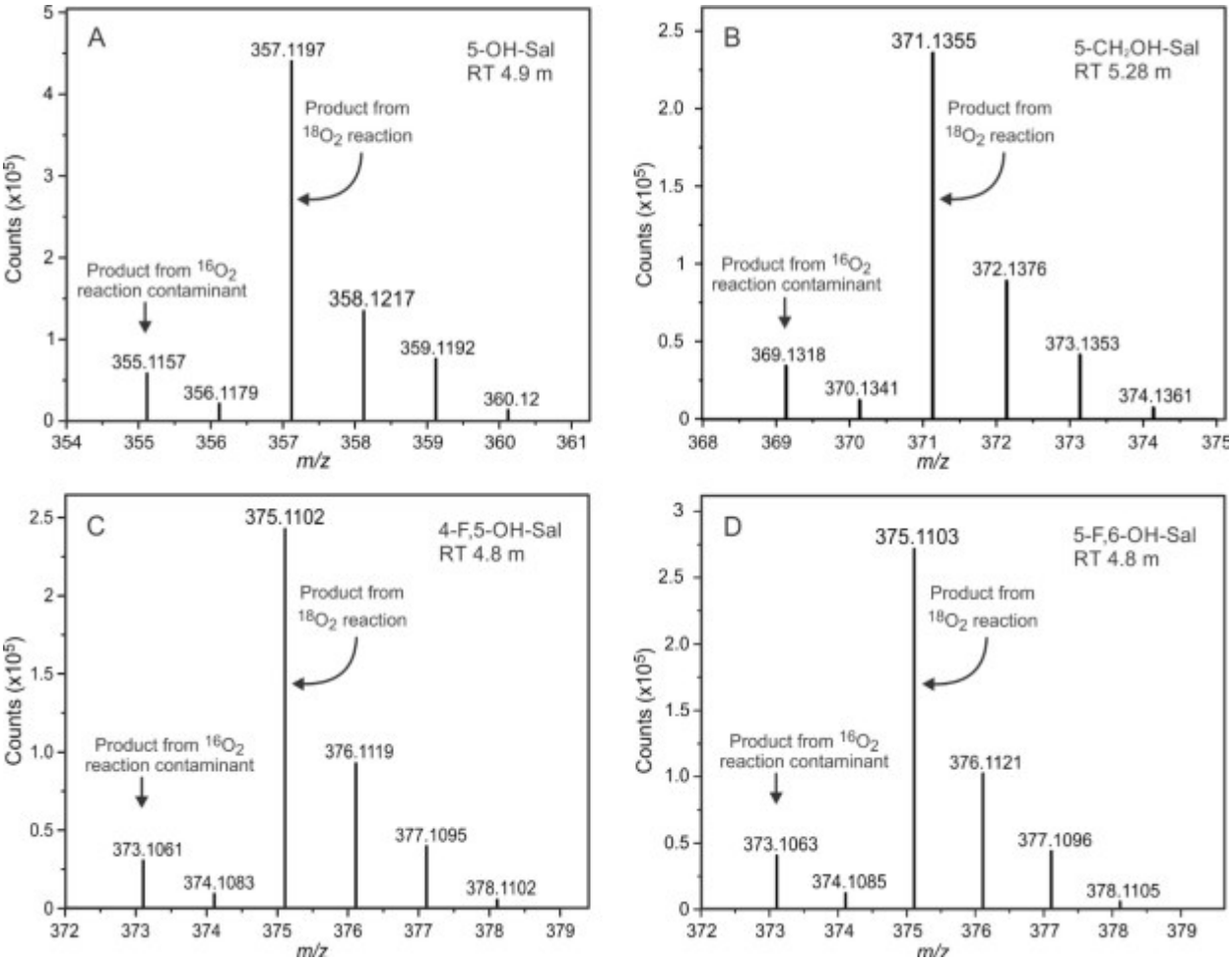

Figure 5. The oxygen atom incorporated into the product originates from O_2. Mass spectra of the TMS-derivatives of products from single turnover reaction of S5HH using $^{18}O_2$ with (A) salicylate, (B) 5-CH_3-Sal, (C) 4-F-salicylate and (D) 5-F-salicylate. The mass species corresponds to the parent TMS derivative minus a methyl group. RT = GC retention time. Reaction conditions are given in Experimental Procedures.

Table 2. Incorporation of ^{18}O into the Reaction Products from Single Turnover Reactions of S5HH

Substrate[a]	Product ^{18}O (%)[b]	
	$^{18}O_2$ / $H_2{}^{16}O$	$^{16}O_2$ / $H_2{}^{18}O$
salicylate	86.35	0
5-CH_3-salicylate	85.15	0
4-F-salicylate	86.99	not tested
5-F-salicylate	86.89	not tested

[a]Reaction conditions are given in Experimental Procedures
[b]GCMS detection

Kinetic Isotope Effects Differ for Aromatic Hydroxylation Versus Aryl-Methyl Substituent Hydroxylation. Stopped-flow experiments were performed using deuterated substrates as mechanistic probes to determine whether any individual catalytic step up to and including electron transfer from the Rieske cluster exhibits a rate-limiting KIE (Figure 6). The reciprocal relaxation times were compared for the first (product forming) phases of single turnover reactions of unlabeled and deuterium labeled substrates. The salicylate reaction ($1/\tau_1$ salicylate / $1/\tau_1$ salicylate-*d*$_6$) exhibited no KIE within error (KIE = 1.02 ± 0.04). In contrast, the 5-CH_3-Sal reaction ($1/\tau_1$ 5-CH_3-Sal / $1/\tau_1$ 5-CD_3-Sal-*d*$_8$) monitored by oxidation of the Rieske cluster exhibited an inverse KIE (KIE = 0.86 ± 0.05). Contamination of 5-CD_3-salicylate-*d*$_8$ with salicylate would be one means to account for this unexpected observation, but the method used to synthesize the deuterated substrate by the supplier obviates this possibility and no salicylate was found experimentally in HPLC samples.

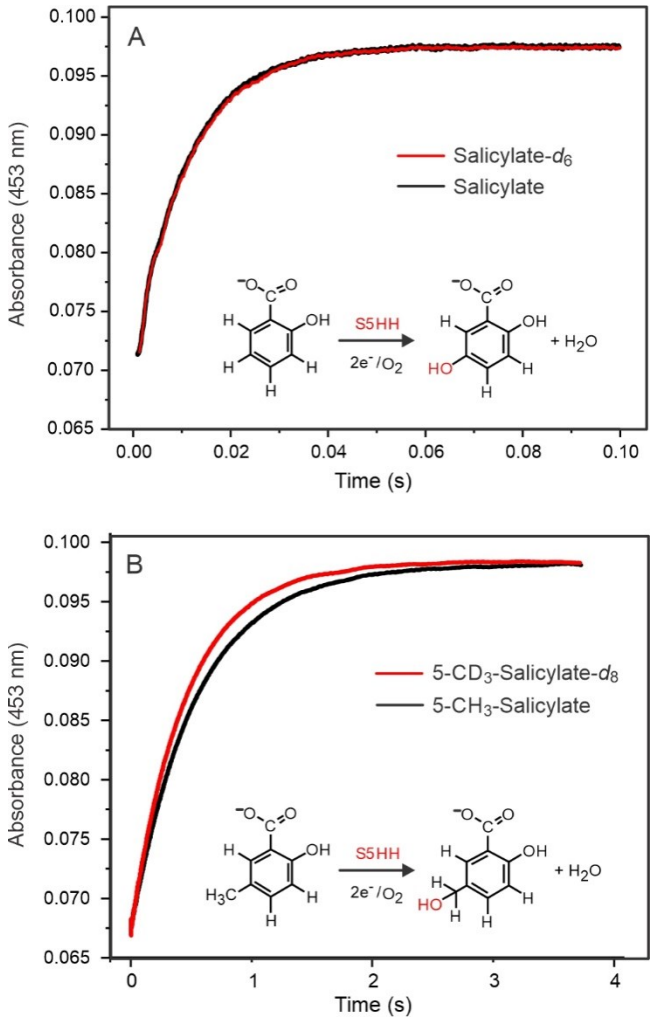

Figure 6. Deuterium kinetic isotope effects observed when monitoring the Rieske electron transfer step in a single turnover reaction. (A) salicylate or salicylate-d_6 as the substrate and (B) 5-CH_3-salicylate or 5-CD_3-salicylate-d_8 as the substrate. Reduced S5HH (30 μM) was reacted with individual substrates (5 mM) and O_2 (900 μM) (Concentrations after mixing) at 4 °C in 50 mM HEPES, 100 mM NaCl, 5 % glycerol, pH 8.0. Time courses were fitted by nonlinear regression using a summed three exponential expression. The fastest kinetic phase in which product is formed was extracted from the data and plotted in each case.

Product Isotope Effects Differ for Aromatic Hydroxylation versus Ring Methyl Substituent Hydroxylation. The reaction cycle of S5H is strongly rate limited by product release, thus determination of a product KIE by sampling during steady state turnover could not be employed. Single turnover experiments were conducted using equimolar mixtures of salicylate and salicylate-d_6 or 5-CH_3-Sal and 5-CD_3-Sal-d_8 as the substrate, and then the products extracted and analyzed by GCMS. While no product IE within error was observed for

salicylate hydroxylation (see Discussion), methyl hydroxylation of 5-CH_3-Sal exhibited a value of 1.55 ± 0.04 (Figure 7 and Table 3).

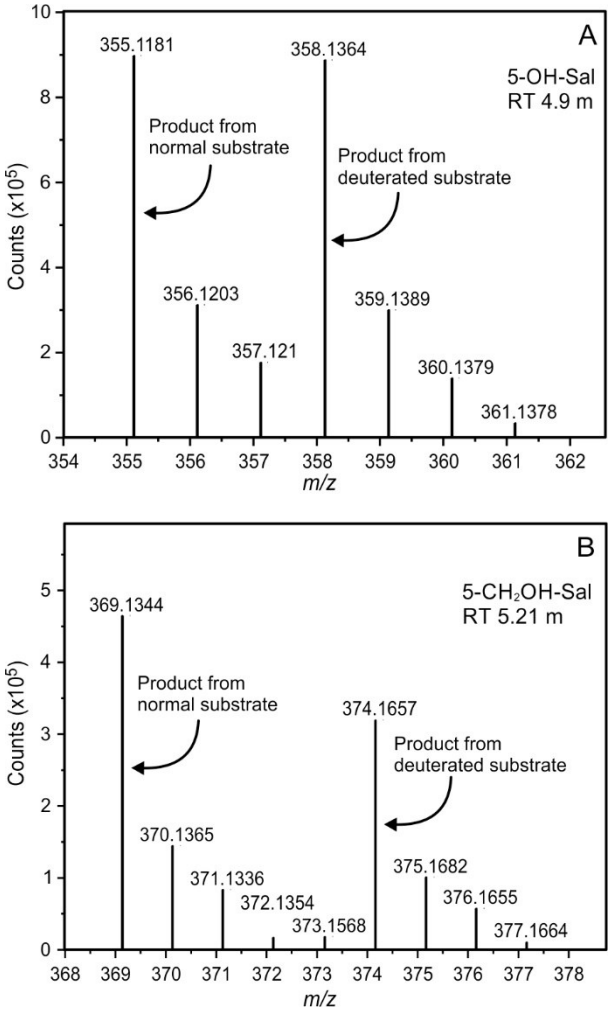

Figure 7. Product isotope effect determined from mass spectrometry analysis of products from single turnover reaction of S5HH with (A) equimolar salicylate and salicylate-d_6 or (B) equimolar 5-CH_3-salicylate and 5-CD_3-salicylate-d_8. RT= GC retention times. Reaction conditions are given in Experimental Procedures.

Table 3. Kinetic and Product Isotope Effects for Single Turnover Reaction of S5HH with Salicylate and 5-Methyl-Salicylate.[a]

Substrate	Isotope Effect	
	Kinetic IE	Product IE
salicylate	1.02 ± 0.04	1.03 ± 0.03
5-methyl-salicylate	0.86 ± 0.05	1.55 ± 0.04

[a]Reaction conditions are given in Experimental Procedures

Computed Substrate Atomic Charge. Previous studies of the mechanism of cis-diol forming benzoate 1,2-dioxygenase showed that the position of attack by the activated oxygen species occurred at the ring carbon with the largest atomic charge. The atomic charges at each carbon for the (unbound) substrates for S5H studied here were computed using the methods described in Experimental Procedures. Inspection of the active site of an S5HH-salicylate complex modeled from the crystal structure indicates that ring carbons 4 through 6 of the bound substrate will be closest to the iron (see below).[59] The atomic charges for the ring carbons 4 to 6 are listed in Table 1 and values for all carbons are shown in Figures S15-S17. The computed bond dissociation energies for specific bonds of interest are listed in Table S1 and the electrostatic potential surface maps are shown graphically in Figure 8. While the data supports reaction at the substrate carbon facing the mononuclear iron site with the largest atomic charge for S5H monooxygenase, the correlation with reaction rate is more complex than found for the cis-diol forming dioxygenase,[84] as discussed below.

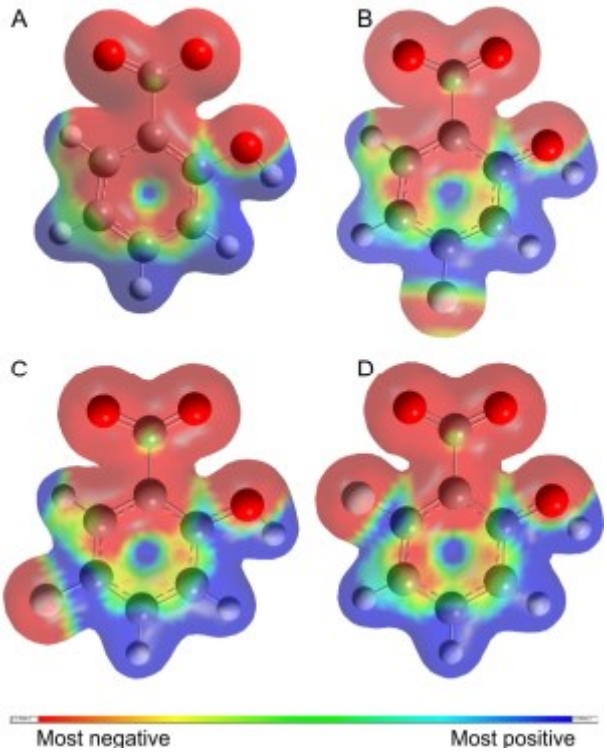

Figure 8. Electrostatic potential surface maps of (A) salicylate and (B) 4-F-salicylate, (C) 5-F-salicylate and (D) 6-F-salicylate (computed with GaussView 6.1).[122]

DISCUSSION

The current study shows that a dedicated Rieske monooxygenase with no detectable dioxygenase activity exhibits dramatic sensitivity to the electronic structure of the substrate in the rate constant of electron transfer from the Rieske cluster to the reactive mononuclear iron site. In particular, the rate constant is greatly decreased by the inclusion of electron withdrawing fluorine substituents, mimicking findings for Rieske dioxygenases.[78, 84] It is also confirmed by direct product analysis that the chemical reaction catalyzed by S5HH switches quantitatively from aromatic hydroxylation to methyl hydroxylation when a methyl substituent is placed in the normal position of hydroxyl incorporation on the aromatic ring. Unexpectedly, Rieske cluster oxidation kinetics and product formation exhibit opposite deuterium isotope effects during the methyl substituent hydroxylation reaction, offering new insight into the mechanism(s) of Rieske monooxygenation. These findings are discussed here in the context of structural, kinetic, and mechanistic studies of enzymes in the broad Rieske oxygenase family.

Correlation of Rieske Monooxygenase Activity with Substrate Atomic Charge in Aromatic Ring Hydroxylation. The recent publication of the X-ray crystal structure of S5HH and computational docking of substrate in the active site by Li, Zhou and co-workers[59] (illustrated in Figure 9) suggested three important aspects of the active site: (i) substrate binds near, but not to, the mononuclear Fe(II), (ii) the substrate is fixed in place by hydrophobic interactions with the ring, electrostatic or hydrogen bonding of the carboxylate substituent with Arg323 and Gln316, and hydrogen bonding of salicylate C2-OH with Ser367, and (iii) the position of the ring places salicylate C5 closest to the iron (~ 4.0 Å) with C6 and C4 only slightly more distant (~ 4.1 Å). The S5HH crystal structure represents a static picture of the active site with the metals in a single oxidation state. However, during catalysis, both metal centers change redox state,[108] and there are likely to be substantial changes to the relative positions of the metal centers and substrate as the reaction cycle progresses. The latter hypothesis is based on studies of three Rieske cis-diol forming dioxygenases with nearly identical structures to S5HH in terms of iron ligation and the cross-subunit boundary connection to the Rieske cluster. It was shown that the distance between the mononuclear iron and the closest substrate carbon is modulated by the oxidation state of the Rieske cluster.[68, 80, 129, 130] The distance decreases as the mononuclear iron shifts toward the substrate when the cluster is in the oxidized state. The mechanism we proposed for S5HH (Scheme 2) suggests that reduction of the Rieske

cluster shifts the mononuclear iron and the substrate apart, thereby opening sufficient space for O_2 to bind to the iron in an end-on conformation to form an Fe(III)-superoxo adduct. This binding mode allows electrophilic attack on the closest ring carbon, C5 in the case of S5HH, which is also the carbon with the most negative atomic charge of those facing the mononuclear iron (Table 1, Figures 8, 9 and S15-S17).

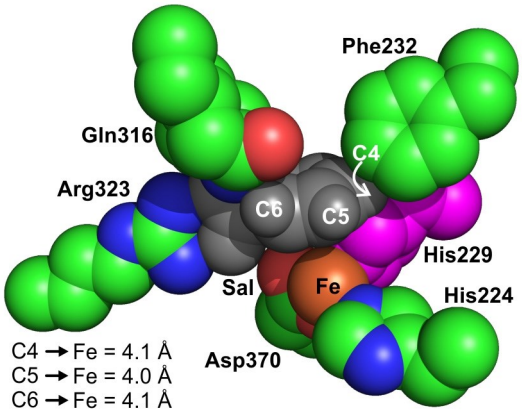

Figure 9. Salicylate C4 is occluded from the iron in the active site model of an S5HH:salicylate (grey) substrate complex.[59] Ser367, which hydrogen bonds to the salicylate C2 hydroxyl, is behind salicylate in this orientation. His229 (magenta) lies between salicylate C4 and the iron. Salicylate C5 and C6 are not occluded. Distances between the selected salicylate carbons and the iron are show on the figure. Derived from PDB ID: 7C8Z.

The same S5H mechanism can be written for the salicylate and benzoate derivatives with fluorine substituents, as illustrated in Scheme 3. The fluorine withdraws electron density from the ring, slowing the attack by the metal-bound superoxo, but C5 still possesses the most negative charge of the ring carbons closest to the iron (C4, C5, and C6). Placement of the fluorine at C5 of salicylate is found to shift the position of hydroxylation to C6. Indeed, the atomic charge computations show that C5 is strongly deactivated while C4 and C6 now have the most negative charge (Table 1, Figures 8 and S16). In the model of the S5HH:salicylate substrate complex, C4 is adjacent to Phe232 and largely occluded from the oxygen binding site on the iron by the iron ligand His229 (Figure 9). This geometry may direct attack of the metal-superoxo to the unblocked C6. It is notable that aromatic ring hydroxylation also does not occur at C3 despite substantial negative charge, supportive of the docking model, where this position would also be distal from the mononuclear iron. The docking model is similarly supported by the observation that 3-CH_3-benzoate is hydroxylated only on the methyl substituent (Table 1) despite substantial negative charge on the C4-C6 ring carbons (Table 1, Figure S17). This finding suggests that the

methyl can only be accommodated in the active site in the same orientation as the C5-methyl of 5-CH_3-Sal, and in this position, C6-C4 ring carbons are far from the iron.

Scheme 3. **Proposed Mechanism of S5HH when a Fluorine Substituent is Present**[a]

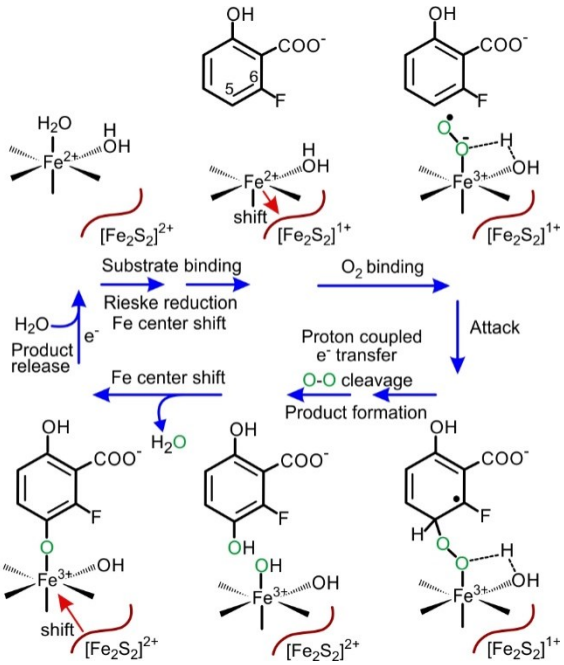

[a]O-O bond cleavage may require intermediate arene oxide formation, although no fluorine NIH shift is observed.

Our current results support a model in which an Fe(III)-superoxo species attacks the ring at the closest carbon with the most negative charge as proposed for the Rieske dioxygenase class. However, we do not find the linear correlation between the log of the fastest reciprocal relaxation time and the atomic charge at the carbon where attack occurs as seen for the Rieske dioxygenase benzoate 1,2-dioxygenase using a range of fluorinated benzoates.[84] This finding presumably reflects effects of the active site to block access of the reactive species to specific ring carbons and/or control of bonding interactions with certain ring substituents. This hypothesis is consistent with the >20-fold difference in first phase $1/\tau_1$ values observed for 4-F- and 6-F-salicylate substrates without a change in atomic charge at C5 (Table 1). However, the true origin of the kinetic effects will require structural studies of the substrate complexes and more in-depth computations of the molecular mechanism.

Comparison of the Mechanisms of Rieske Mono- and Di- Oxygenases. The question of where the proposed mechanisms for Rieske cis-dihydroxylation and aromatic hydroxylation diverge remains unresolved. Our current proposal is that both mechanisms follow

the same course up through Rieske electron transfer. Computations for the dioxygenase mechanism in BZDO show that O-O bond cleavage in the resulting Fe(III)-peroxo-aryl intermediate would be very energetically favorable when electron and proton transfer are coupled.[82] In the computed model, the cis-diol formation proceeds through an epoxide intermediate, which is commonly proposed for electrophilic aromatic hydroxylation (Scheme 4).[88-90, 131] Such reactions sometimes involve an NIH shift, generally manifesting as an internal hydride transfer to an intermediate carbocation formed during epoxide ring opening. However, to yield cis-dihydrodiol products, this process would instead require transfer of the second oxygen from the O_2, nominally bound as Fe(III)-OH (Scheme 4). If the substrate orientation was unsuitable for this capture, then the intermediate might decay by the normal NIH shift hydride transfer to yield a monohydroxylation product. Such critical dependence on substrate positioning would account for the observation that some Rieske dioxygenases can also catalyze monooxygenase reactions with alternative substrates.[5, 75, 97]

Scheme 4. A Proposal for a Common Intermediate for Rieske Monooxygenase and Dioxygenase Reactions

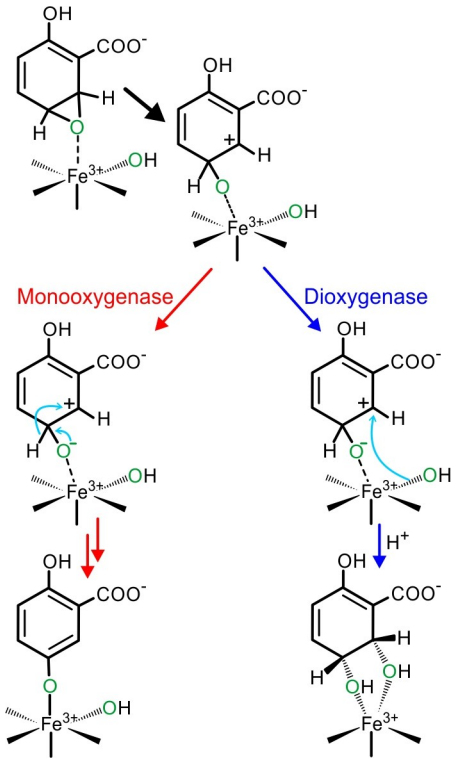

It is also possible that ring hydroxylation in the case of the dedicated Rieske monooxygenase involves oxygen transfer without intermediate epoxide formation as proposed

for some oxygenases,[90, 132] and consequently, no NIH shift would be expected. While the presence or absence of a deuterium NIH shift has not been evaluated for a Rieske monooxygenase, the current results show that there is no fluorine shift or elimination in the S5H reaction. In contrast, in other heme and non-heme iron oxygenases, fluorine shift or defluorination is observed for aromatic substrates that are proposed to form epoxide intermediates including cytochrome P450, 2-halobenzoate-1,2-dioxygenase and tyrosine hydroxylase.[90, 133-140]

Comparison of Isotope Effects for Ring and Methyl Substituent Hydroxylation. The studies reported here demonstrate that O_2 is the only source of oxygen for both aromatic ring and methyl substituent hydroxylations. Thus, S5HH functions as an oxygenase in each case. In general, oxygenase reactions with aromatic rings do not involve direct hydrogen abstraction due to the strength of the C-H bonds involved (BDFE = 101-106 kcal/mol., Table S1),[141] and thus, a large primary deuterium isotope is not expected. A smaller secondary isotope effect may be observed for a mechanism in which an electrophilic Fe(III)-superoxo intermediate directly attacks the aromatic ring (see, for example, Schemes 2 and 3) due to changes in zero-point energies for C-H versus C-D as the aromatic carbon changes hybridization. When observed, this isotope effect is inverse, indicating that the deuterated substrate reacts more rapidly.[142] As shown in Figure 6, no KIE is observed when monitoring the time course of Rieske oxidation during the ring hydroxylation of salicylate. However, small KIE effects are difficult to observe in transient experiments of very fast reactions due to signal-to-noise limitations. In contrast, an inverse KIE value is observed when monitoring the time course of the relatively slow Rieske oxidation during the methyl substituent hydroxylation reaction when using 5-CH_3-Sal as the substrate. This result is unexpected if it is associated in any direct way with breaking the C-H bond of the methyl substituent. The strength of this bond is much less than that of the aromatic C-H bond (BDFE = 81.4 kcal/mol., Table S1), but its cleavage still requires a powerful oxidizing intermediate such as a Fe(IV)-oxo, Fe(V)-oxo, or perhaps Fe(III)-hydroperoxo.[94, 141, 143] Direct cleavage of the methyl C-H bond by these species would yield a normal rather than inverse KIE.[144]

One intriguing hypothesis for the origin of the inverse KIE on Rieske oxidation is illustrated in Scheme 5. It is proposed that methyl substituent hydroxylation reaction must begin in the same way as aromatic ring hydroxylation. The electron from the Rieske cluster is required

to generate a reactive species, but it cannot be transferred to the already reduced Fe(II) site. Binding of O_2 to the iron begins its oxidation process, but the iron only becomes fully oxidized and able to accept the Rieske electron after attack on the aromatic ring by the Fe(III)-superoxo intermediate. Accordingly, the ring carbons at C4, C5, and C6 of 5-CH_3-Sal retain the net negative charge required for such an attack (Table 1, Figure S15). As in the case of aromatic ring hydroxylation, this reaction is rate-limiting in the sequence of reactions leading to electron transfer from the Rieske cluster. It is interesting to note that no Rieske oxidation above that expected for autooxidation occurs when 5-CF_3-Sal is bound in the active site (Figure 4). Accordingly, computation of the atomic charges for 5-CF_3-Sal shows that C4 and C6 are strongly deactivated for attack by the putative Fe(III)-superoxo intermediate, while the bulky methyl substituent prevents attack at C5 (Table 1, Figure S15).

Understanding the basis for the remaining steps in the mechanism proposed in Scheme 5 requires examination of the methods used to determine the product isotope effect. The overall reaction of S5H is strongly rate-limited by product dissociation.[108] Consequently, methods to determine isotope effects such as reaction sampling during steady-state turnover are complex. Similarly, the very rapid product formation after Rieske oxidation during ring hydroxylation does not permit sampling during the course of a single turnover. Such sampling might be possible during the single turnover methyl-substituent reaction (Figure 3B), but the close correlation between product formation and Rieske oxidation suggests a very short lifetime for any intermediate that might be definitive. Indeed, our initial attempts to find an intermediate using rapid trapping techniques have been unsuccessful. Unfortunately, the method employed here of sampling at the end of a single turnover reaction is not definitive for the salicylate aromatic ring hydroxylation reaction, because no product isotope effect is observed when equal concentrations of labeled and unlabeled substrate are present at the beginning of the reaction. Lack of an observed product isotope effect could mean that the presence of deuterium actually has no effect on the rate of product formation, as expected when the deuterium is bound to ring carbons. Alternatively, there may be an appreciable isotope effect from deuterium which is masked by a failure of the substrate to dissociate once bound. In a single turnover reaction, a non-dissociating substrate will result in an isotopic distribution in the products which mirrors that in the substrate mixture. In contrast, the observation of a deuterium isotope effect in the case of aromatic methyl-substituent hydroxylation in a single turnover reaction has substantial

ramifications for the reaction chemistry. First, it indicates that there is a normal product isotope effect that is at least as large as that observed, supportive of direct hydrogen abstraction. Second, it requires that the substrates be able to exchange from solution into the active site up to the point of irreversible reaction, presumably hydrogen abstraction from the substituent methyl group. If this were not the case, then the isotope ratio in the product would be the same as that in the substrate in solution at the start of the reaction, i.e. 1:1. Third, the substrate exchange must be fast compared with product formation. Fourth, the apparent correlation between product formation and $1/\tau_1$ of the Rieske oxidation time course (when a two-electron reduced oxygen species is formed that is capable of substrate hydroxylation) suggests that product formation must be fast compared with the steps that rate limit the observed electron transfer (Figure 3B). Note that the rate constant for the electron transfer itself through bonds across 12 Å would exceed any of the rate constants reported here by many orders of magnitude.[82, 145] This fact makes it unlikely that a simple change in redox potential of the mononuclear iron caused by an environmental change due to the substitution of a fluorine on the substrate ring would alter the *observed* electron transfer rate constant.

In the case of S5H, substrate binding at the beginning of the reaction cycle is very fast relative to observed Rieske oxidation,[108] supporting the notion that exchange in the short time period between electron transfer and irreversible hydrogen atom abstraction may be possible. Additionally, the hydroxyl radical rebound reaction in non-heme oxygenases is known to be very fast, typically occurring six or more orders of magnitude faster than the $1/\tau_1$ for Rieske cluster oxidation observed for S5HH.[95, 146, 147]

The requirement for substrate exchange after O_2 activation, but before irreversible reaction with the substrate implies that the proposed preceding Fe(III)-peroxo-substrate intermediate must be reversibly formed, at least for slow substrates like 5-CH_3-Sal. For example, the stability of this intermediate might be affected due to perturbation of its position in the active site by the bulky methyl substituent. Similar shifts in precise alignment and reaction outcome are observed in other oxygenases after minor changes in substrate structure.[148] Reversal of the ring C-O bond formation without reverse of Rieske electron transfer against a steep redox potential gradient[124, 125] would yield a comparatively stable Fe(III)-(hydro)peroxo intermediate. Moreover, the shift of the mononuclear iron toward the substrate that is associated with an oxidation of the Rieske cluster would be maintained.[68, 80, 129, 130] In the case of BZDO, the H_2O_2 complex of the

fully oxidized enzyme results in side-on rather than end-on H_2O_2 binding.[85] A shift from end-on to side-on bound (hydro)peroxo in S5HH might also be promoted by the bulk of the methyl substituent in the space near the iron (Scheme 5). This type of intermediate is predicted computationally to progress with almost no energy barrier to a reactive HO-Fe(V)=O species.[82] The HO-Fe(V)=O species, now forced close to the aromatic methyl substituent by the shift in the mononuclear iron position, could readily abstract a methyl hydrogen atom from the substrate.[113] Hydroxylation chemistry would then proceed via the well characterized hydroxyl radical rebound mechanism observed for P450 and methane monooxygenase oxygenases.[146, 149, 150] Hydrogen atom abstraction by a high-valent iron-oxo species with substrate radical intermediate formation is consistent with radical clock experiments in which the Rieske dioxygenase naphthalene 1,2-dioxygenase catalyzes monooxygenation of probe molecules.[95] In this reaction, a radical intermediate with a lifetime of ~18 ns was formed prior to rearrangement of the probe molecule to diagnostic products.

Scheme 5. A Potential Mechanism for Methyl Substituent Hydroxylation by S5HH[a]

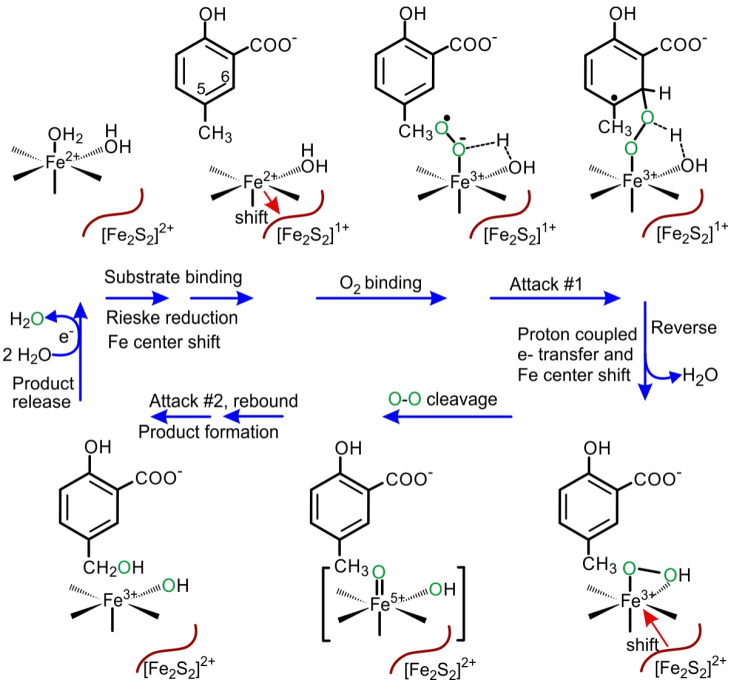

[a]The Fe(V)=O intermediate shown is one of several possible activated oxygen species at this stage of the reaction cycle.

Alternative Proposals for Rieske Oxygenase Mechanisms. The proposal here for shared *initial* steps in the O_2 activation and substrate reactions of Rieske dioxygenases and monooxygenases (compare Schemes 3, 4 and 5) can be examined in the broader context of other mechanisms proposed for the Rieske oxygenase family. We have previously discussed many of

the potential mechanisms involving high valent, peroxo, or dioxetane intermediates formed after the electron from Rieske cluster has been transferred to the mononuclear iron site.[84, 108] These types of mechanisms are largely ruled out for the initial attack by an activated oxygen species on the substrate by the consistent observation that the type and electronic character of substrate dictate the rate constant for transfer of the Rieske electron.[78, 84, 108] Nevertheless, a recent detailed study of the reaction of the Rieske dioxygenase nitrobenzene dioxygenase (NBDO) by Hofstetter and co-workers, used $^{18}O_2$ to show that the $^{16}O/^{18}O$-kinetic isotope effects (^{18}O-KIE) for a range of substrates were both similar to each other and approached the ^{18}O-equilibrium isotope effect (^{18}O-EIE) expected for an Fe(III)-(hydro)-peroxo species participating in the rate-determining step of the reaction with substrate.[81] The ^{18}O-KIE must be less than or equal to the ^{18}O-EIE for any reaction,[151-153] and the observed ^{18}O-KIE for the NBDO reactions significantly exceeds the literature value for the ^{18}O-EIE value for the Fe(III)-superoxo species found in hemoglobin and myoglobin. While the ^{18}O-KIE method is very sensitive, it is limited in the case of Rieske oxygenases by: (i) the presence of three parallel substrate-dependent Rieske cluster oxidation reactions, only one of which results in product formation,[84, 108] and (ii) the unknown ^{18}O-EIE for the type of Fe(III)-superoxo species proposed for Rieske oxygenases, which is coupled through bonds to the reduced Rieske cluster.[59, 154] Also, the ^{18}O-KIE is reflective of the rate determining step of the relative k_{cat}/K_m values for the reactions using $^{18}O_2$ and $^{16}O_2$. The k_{cat}/K_m value is composed of rate constants up to and including the first irreversible step in the reaction sequence, which may or may not be rate determining.[155] Our study suggests that the formation of the Fe(III)-peroxo-bridged aryl intermediate is reversible, at least for some slow substrates. Thus, the actual first irreversible step would occur later in the cycle, and the kinetics of the Fe(III)-peroxo-bridged aryl intermediate formation and decay would be reflected, at least in part, in the ^{18}O-KIE. The ^{18}O-EIE for such a complex has not been determined, but that for the similar Fe(III)-peroxo bridged-tert-butyl complex is known and has a value[153, 156, 157] nearly identical to that of the Fe(III)-(hydro)-peroxo proposed as the alternative initial reactive species.[94, 128, 143]

While attack on the substrate by an Fe(III)-superoxo intermediate prior to Rieske cluster oxidation appears to provide the most direct explanation for the observed single turnover kinetics, the downstream reactions are less well defined. Electron transfer to the proposed Fe(III)-peroxo-substrate radical intermediate would yield a species in which the O-O bond could

be readily broken by any of several routes. Indeed, different routes may be employed by the Rieske oxygenases in response to the metabolic challenges presented.

■ CONCLUSIONS

The current results support a mechanism for Rieske monooxygenases that can proceed along more than one pathway depending upon the type and electronic properties of the substrate. For S5HH with both metal centers reduced, the natural substrate, salicylate, can bind in the proper alignment to allow rapid O_2 binding to the mononuclear iron to form an Fe(III)-superoxo intermediate. Salicylate also has the correct charge distribution to be rapidly attacked by this activated oxygen species, ultimately creating a fully oxidized mononuclear iron that can accept an electron from the Rieske cluster to complete the oxygen activation process. In the broader context of regulation in oxygenase reactions, these steps insure that O_2 is only activated: (i) after substrate is correctly bound, (ii) O_2 is bound to the mononuclear iron adjacent to the substrate, and (iii) both electrons required to complete the reaction are present in the enzyme. Once both electrons are transferred to the bridged Fe(III)-peroxo-substrate complex, the hydroxylation reaction could proceed by the well-established steps of electrophilic aromatic substitution. However, the current results introduce two potential variations. First, the lack of fluorine shift or elimination when present at or adjacent to the position of hydroxylation raises the possibility of a mechanism without formation of the arene-oxide common to electrophilic aromatic substitution. Second, the substrate exchange after oxygen activation required to explain the observed product isotope effect for substituent hydroxylation of 5-CH_3-Sal suggests that a Fe(III)-(hydro)peroxo intermediate, not bound to the substrate, may be formed after the initial Fe(III)-peroxo-aryl-radical intermediate. Such an intermediate might directly reattack the substrate for hydroxylation or dioxygenation akin to the mechanism favored in some past studies.[94, 128, 143] Alternatively, it might convert to an HO-Fe(V)=O species capable of chemistry requiring a more energetic species. The route taken by any given Rieske oxygenase after the initial substrate-coupled activation steps is likely to be controlled by the precise electronic properties and positioning of the substrate, and ultimately, the kinetics of reaction with substrate. The reciprocal relaxation times of these reactions have been shown to differ by over 2 orders of magnitude even within a single enzyme. Given their conserved active site structure, it seems likely that all Rieske

oxygenases have the potential for this multi-pathway reactivity, which may account for the remarkable diversity of chemistry that they exhibit.

■ ASSOCIATED CONTENT

Supporting Information

The Supporting Information is available free of charge on the ACS Publications website at DOI:. Additional experimental procedures, Table S1, and Figures S1−S17 (PDF)

Accession Codes

S5H oxygenase (S5HH), UniProt entries O52379 and O52380

■ AUTHOR INFORMATION

Corresponding Author

John D. Lipscomb - *Department of Biochemistry, Molecular Biology, and Biophysics and Center for Metals in Biocatalysis, University of Minnesota, Minneapolis, Minnesota 55455, United States*; orcid.org/0000-0002-8158-5594; Email: Lipsc001@umn.edu

Authors

Melanie S. Rogers - *Department of Biochemistry, Molecular Biology, and Biophysics and Center for Metals in Biocatalysis, University of Minnesota, Minneapolis, Minnesota 55455, United States*; orcid.org/0000-0002-2657-7065; Email: roger282@umn.edu

Adrian Gordon - *Department of Chemistry, University of Minnesota, Minneapolis, Minnesota 55455, United States*; orcid.org/0000-0002-8027-2633; Email: gordo766@umn.edu

Todd M. Rappe - *Minnesota NMR Center, University of Minnesota, Minneapolis, Minnesota 55455, United States*; orcid.org/0000-0002-1510-553X; Email: rapp0006@umn.edu

Jason D. Goodpaster - *Department of Chemistry, University of Minnesota, Minneapolis, Minnesota 55455, United States*; orcid.org/0000-0001-6461-4501; Email: jgoodpas@umn.edu

Notes

The authors declare no competing financial interest.

■ ACKNOWLEDGMENTS

The authors acknowledge financial support of this work from National Institutes of Health (NIH) Grant GM118030 (to J.D.L.) and the National Science Foundation Grant No. CHE-1945525 (to J. D. G.). Mass spectrometry analysis was performed at The University of Minnesota Department of Chemistry Mass Spectrometry Laboratory, supported by the Office of the Vice President of Research, College of Science and Engineering, and the Department of Chemistry at the University of Minnesota, as well as the National Science Foundation Award CHE-1336940. ^{1}H NMR spectroscopy at the UMN Chemistry NMR Laboratory was supported by the Office of the Vice President of Research, College of Science and Engineering, and the Department of Chemistry at the University of Minnesota. Structures of fluorinated S5HH reaction products were determined using the University of Minnesota NMR Center supported by from NIH Grant 1S10OD021536. The authors acknowledge the Minnesota Supercomputing Institute (MSI) at the University of Minnesota and the National Energy Research Scientific Computing Center (NERSC), a DOE Office of Science User Facility supported by the Office of Science of the U.S. Department of Energy under Contract DE-AC02-05CH11231. The authors thank Sean Murray and Joseph Dalluge for assistance with GCMS data collection and analysis. The authors thank Letitia Yao and Phillipe Buhlmann for insightful discussions regarding the 5-hydroxylmethyl-salicylate and 3-hydroxylmethyl-benzoate S5HH reaction product determination via ^{1}H NMR. The authors thank De-Feng Li for generously providing the salicylate-bound structural model of salicylate 5-hydroxylase (derived from PDB ID: 7C8Z).

■ REFERENCES

[1] Guo, Y., Chang, W.-c., Li, J., and Davidson, M. (2021) Non-heme mono-iron enzymes: Co-substrate-independent dioxygen activation, In *Comprehensive Coordination Chemistry III* (Constable, E. C., Parkin, G., and Que Jr, L., Eds.), pp 301-332, Elsevier, Oxford.

[2] Knapp, M., Mendoza, J., and Bridwell-Rabb, J. (2021) An aerobic route for C-H bond functionalization: The Rieske non-heme iron oxygenases, In *Encyclopedia of Biological Chemistry III (Third Edition)* (Jez, J., Ed.), pp 413-424, Elsevier.

[3] Vila, M. A., Pazos, M., Iglesias, C., Veiga, N., Seoane, G., and Carrera, I. (2016) Toluene dioxygenase-catalysed oxidation of benzyl azide to benzonitrile: Mechanistic insights for an unprecedented enzymatic transformation, *Chembiochem 17*, 291-295.

[4] Vila, M. A., Steck, V., Rodriguez Giordano, S., Carrera, I., and Fasan, R. (2020) C-H amination via nitrene transfer catalyzed by mononuclear non-heme iron-dependent enzymes, *ChemBioChem 21*, 1981-1987.

[5] Resnick, S. M., Lee, K., and Gibson, D. T. (1996) Diverse reactions catalyzed by naphthalene dioxygenase from *Pseudomonas* sp. strain NCIB 9816, *J. Ind. Microbiol. Biotechnol. 17*, 438-457.
[6] Hudlicky, T., Gonzalez, D., and Gibson, D. T. (1999) Enzymatic dihydroxylation of aromatics in enantioselective synthesis: Expanding asymmetric methodology, *Aldrichimica Acta 32*, 35-62.
[7] Barry, S., and Challis, G. L. (2013) Mechanism and catalytic diversity of Rieske non-heme iron-dependent oxygenases, *ACS Catal. 3*, 2362–2370.
[8] Ferraro, D. J., Gakhar, L., and Ramaswamy, S. (2005) Rieske business: Structure-function of Rieske non-heme oxygenases, *Biochem. Biophys. Res. Commun. 338*, 175-190.
[9] Peng, R.-H., Xiong, A.-S., Xue, Y., Fu, X.-Y., Gao, F., Zhao, W., Tian, Y.-S., Yao, Q.-H., and Whitacre, D. M. M. (2010) A profile of ring-hydroxylating oxygenases that degrade aromatic pollutants, *Rev. Environ. Contam. Toxicol. 206*, 65-94.
[10] Wandi, B. N., Siitonen, V., Palmu, K., and Metsä-Ketelä, M. (2020) The Rieske oxygenase SnoT catalyzes 2"-hydroxylation of L-rhodosamine in nogalamycin biosynthesis, *ChemBioChem 21*, 3062-4066.
[11] Capyk, J. K., and Eltis, L. D. (2012) Phylogenetic analysis reveals the surprising diversity of an oxygenase class, *J. Biol. Inorg. Chem. 17*, 425-436.
[12] Schlenzka, W., Shaw, L., Kelm, S., Schmidt, C. L., Bill, E., Trautwein, A. X., Lottspeich, F., and Schauer, R. (1996) CMP-N-acetylneuraminic acid hydroxylase: the first cytosolic Rieske iron-sulphur protein to be described in Eukarya, *FEBS Lett. 385*, 197-200.
[13] Bergfeld, A. K., and Varki, A. (2014) Cytidine monophospho-N-acetylneuraminic acid hydroxylase (CMAH), In *Handbook of Glycosyltransferases and Related Genes* (Taniguchi, N., Honke, K., Fukuda, M., Narimatsu, H., Yamaguchi, Y., and Angata, T., Eds.), pp 1559-1580, Springer Japan, Tokyo.
[14] Pruzinska, A., Tanner, G., Anders, I., Roca, M., and Hortensteiner, S. (2003) Chlorophyll breakdown: pheophorbide a oxygenase is a Rieske-type iron-sulfur protein, encoded by the accelerated cell death 1 gene, *Proc. Natl. Acad. Sci. USA 100*, 15259-15264.
[15] Hauenstein, M., Christ, B., Das, A., Aubry, S., and Hortensteiner, S. (2016) A role for TIC55 as a hydroxylase of phyllobilins, the products of chlorophyll breakdown during plant senescence, *Plant Cell 28*, 2510-2527.
[16] Reinbothe, S., Bartsch, S., Rossig, C., Davis, M. Y., Yuan, S., Reinbothe, C., and Gray, J. (2019) A protochlorophyllide (Pchlide) a oxygenase for plant viability, *Front. in Plant Sci. 10*, 593, doi:10.3389/fpls.2019.00593
[17] Tanaka, A., Ito, H., Tanaka, R., Tanaka, N. K., Yoshida, K., and Okada, K. (1998) Chlorophyll a oxygenase (CAO) is involved in chlorophyll b formation from chlorophyll a, *Proc. Natl. Acad. Sci. USA 95*, 12719-12723.
[18] Liu, J., Knapp, M., Jo, M., Dill, Z., and Bridwell-Rabb, J. (2022) Rieske oxygenase catalyzed C–H bond functionalization reactions in chlorophyll b biosynthesis, *ACS Cent. Sci.*, doi:/10.1021/acscentsci.1022c00058.
[19] Rathinasabapathi, B., Burnet, M., Russell, B. L., Gage, D. A., Liao, P. C., Nye, G. J., Scott, P., Golbeck, J. H., and Hanson, A. D. (1997) Choline monooxygenase, an unusual iron-sulfur enzyme catalyzing the first step of glycine betaine synthesis in plants: prosthetic group characterization and cDNA cloning, *Proc. Natl. Acad. Sci. USA 94*, 3454-3458.

[20] Berim, A., Park, J. J., and Gang, D. R. (2014) Unexpected roles for ancient proteins: flavone 8-hydroxylase in sweet basil trichomes is a Rieske-type, PAO-family oxygenase, *Plant J. 80*, 385-395.
[21] Yoshiyama-Yanagawa, T., Enya, S., Shimada-Niwa, Y., Yaguchi, S., Haramoto, Y., Matsuya, T., Shiomi, K., Sasakura, Y., Takahashi, S., Asashima, M., Kataoka, H., and Niwa, R. (2011) The conserved Rieske oxygenase DAF-36/Neverland is a novel cholesterol metabolizing enzyme, *J. Biol. Chem. 286*, 25756-25762.
[22] Sathapondecha, P., Panyim, S., and Udomkit, A. (2017) An essential role of Rieske domain oxygenase Neverland in the molting cycle of black tiger shrimp, *Penaeus monodon*, *Comp. Biochem. Physiol. A Mol. Integr. Physiol. 213*, 11-19.
[23] Yoshiyama, T., Namiki, T., Mita, K., Kataoka, H., and Niwa, R. (2006) Neverland is an evolutionally conserved Rieske-domain protein that is essential for ecdysone synthesis and insect growth, *Development 133*, 2565-2574.
[24] Najle, S. R., Nusblat, A. D., Nudel, C. B., and Uttaro, A. D. (2013) The sterol-C7 desaturase from the ciliate *Tetrahymena thermophila* is a Rieske oxygenase, which is highly conserved in animals., *Mol. Biol Evol. 30*, 1630-1643.
[25] Gibson, D. T., and Parales, R. E. (2000) Aromatic hydrocarbon dioxygenases in environmental biotechnology, *Curr. Opin. Biotechnol. 11*, 236-243.
[26] Lukowski, A. L., Ellinwood, D. C., Hinze, M. E., DeLuca, R. J., Du Bois, J., Hall, S., and Narayan, A. R. H. (2018) C–H hydroxylation in paralytic shellfish toxin biosynthesis, *J. Am. Chem. Soc. 140*, 11863-11869.
[27] Lukowski, A. L., Mallik, L., Hinze, M. E., Carlson, B. M., Ellinwood, D. C., Pyser, J. B., Koutmos, M., and Narayan, A. R. H. (2020) Substrate promiscuity of a paralytic shellfish toxin amidinotransferase, *ACS Chem. Biol. 15*, 626-631.
[28] Lukowski, A. L., Denomme, N., Hinze, M. E., Hall, S., Isom, L. L., and Narayan, A. R. H. (2019) Biocatalytic detoxification of paralytic shellfish toxins, *ACS Chem. Biol. 14*, 941-948.
[29] Chakraborty, J., Suzuki-Minakuchi, C., Okada, K., and Nojiri, H. (2017) Thermophilic bacteria are potential sources of novel Rieske non-heme iron oxygenases, *AMB Express 7*, 17, doi:10.1186/s13568-016-0318-5
[30] Massmig, M., Reijerse, E., Krausze, J., Laurich, C., Lubitz, W., Jahn, D., and Moser, J. (2020) Carnitine metabolism in the human gut: Characterization of the two-component carnitine monooxygenase CntAB from *Acinetobacter baumannii*, *J. Biol. Chem. 295*, 13065-13078.
[31] Quareshy, M., Shanmugam, M., Townsend, E., Jameson, E., Bugg, T. D. H., Cameron, A. D., and Chen, Y. (2020) Structural basis of carnitine monooxygenase CntA substrate specificity, inhibition and inter-subunit electron transfer, *J. Biol. Chem. 296*, 100038, doi:10.1074/jbc.RA120.016019
[32] Shanmugam, M., Quareshy, M., Cameron, A., Bugg, T. D. H., and Chen, Y. (2020) Light-activated electron transfer and catalytic mechanism of carnitine oxidation by Rieske-type oxygenase from human microbiota, *Angew. Chem. Int. Ed. 60*, 4529-4534.
[33] Apte, Z., Richman, J., Almonacid, D., Marquez, V., Araya, I., Alegria, M., Saavedra, M., Gomez, L., Espinoza, J., Gimpel, J., Morales, E., and Ortiz, R. (2019) Rieske-type oxygenase/reductase targeted drugs for diagnostic and treatment of diseases, USPTO, US20190050525A1, Psomagen, Inc.
[34] Kincannon, W. M., Zahn, M., Clare, R., Beech, J. L., Romberg, A., James, L., Bothner, B., Beckham, G. T., McGeehan, J. E., and DuBois, J. L. (2022) Biochemical and structural

characterization of an aromatic ring-hydroxylating dioxygenase for terephthalic acid catabolism, *Proc. Natl. Acad. Sci. U. S. A. 119*, e2121426119, doi:doi:10.1073/pnas.2121426119

[35] Xu, Z.-J., Spain Jim, C., Zhou, N.-Y., and Li, T. (2022) Biodegradation of 3-chloronitrobenzene and 3-bromonitrobenzene by *Diaphorobacter* sp. strain JS3051, *Appl. Environ. Microbiol. 88*, e0243721, doi:10.1128/aem.02437-21

[36] Aukema, K. G., Escalante, D. E., Maltby, M. M., Bera, A. K., Aksan, A., and Wackett, L. P. (2017) In silico identification of bioremediation potential: Carbamazepine and other recalcitrant personal care products, *Environ. Sci. Technol. 51*, 880-888.

[37] Bygd, M. D., Aukema, K. G., Richman, J. E., and Wackett, L. P. (2021) Unexpected mechanism of biodegradation and defluorination of 2,2-difluoro-1,3-benzodioxole by *Pseudomonas putida* F1, *mBio 12*, e0300121, doi:10.1128/mBio.03001-21

[38] Mahto, J. K., Neetu, N., Sharma, M., Dubey, M., Vellanki, B. P., and Kumar, P. (2022) Structural insights into dihydroxylation of terephthalate, a product of polyethylene terephthalate degradation, *J. Bacteriol. 204*, e0054321, doi:10.1128/JB.00543-21

[39] Kim, J. H., Kim, B. H., Brooks, S., Kang, S. Y., Summers, R. M., and Song, H. K. (2019) Structural and mechanistic insights into caffeine degradation by the bacterial N-demethylase complex, *J. Mol. Biol. 431*, 3647-3661.

[40] Hunold, A., Escobedo-Hinojosa, W., Potoudis, E., Resende, D., Farr, T., Syrén, P. O., and Hauer, B. (2021) Assembly of a Rieske non-heme iron oxygenase multicomponent system from *Phenylobacterium immobile* E DSM 1986 enables pyrazon cis-dihydroxylation in *E. coli*, *Appl. Microbiol. Biotechnol. 105*, 2003-2015.

[41] Aukema, K. G., Bygd, M. D., Tassoulas, L. J., Richman, J. E., and Wackett, L. P. (2022) Fluoro-recognition: New *in vivo* fluorescent assay for toluene dioxygenase probing induction by and metabolism of polyfluorinated compounds, *Environ. Microbiol. online ahead of print*, doi:10.1111/1462-2920.16187.

[42] D'Ordine, R. L., Rydel, T. J., Storek, M. J., Sturman, E. J., Moshiri, F., Bartlett, R. K., Brown, G. R., Eilers, R. J., Dart, C., Qi, Y., Flasinski, S., and Franklin, S. J. (2009) Dicamba monooxygenase: Structural insights into a dynamic Rieske oxygenase that catalyzes an exocyclic monooxygenation, *J. Mol. Biol. 392*, 481-497.

[43] Osifalujo, E. A., Preston-Herrera, C., Betts, P. C., Satterwhite, L. R., and Froese, J. T. (2022) Improving toluene dioxygenase activity for ester-functionalized substrates through enzyme engineering, *ChemistrySelect 7*, e202200753, doi:10.1002/slct.202200753

[44] Bedard, K., and Hudlicky, T. (2021) Enzymatic dihydroxylation of aromatic compounds: Nature's unique reaction and its impact on the synthesis of natural products, In *Strategies and Tactics in Organic Synthesis* (Harmata, M., Ed.), pp 53-97, Academic Press.

[45] Wissner, J. L., Escobedo-Hinojosa, W., Vogel, A., and Hauer, B. (2021) An engineered toluene dioxygenase for a single step biocatalytical production of (-)-(1S,2R)-cis-1,2-dihydro-1,2-naphthalenediol, *J. Biotechnol. 326*, 37-39.

[46] Bent, J. S., Clark, Z. T., and Collins, J. A. (2022) Quantitative ^{1}H-NMR analysis reveals steric and electronic effects on the substrate specificity of benzoate dioxygenase in *Ralstonia eutropha* B9, *J. Ind. Microbiol. Biotechnol. 49*, doi:10.1093/jimb/kuac006

[47] Feyza Özgen, F., Runda, M. E., Burek, B. O., Wied, P., Bloh, J. Z., Kourist, R., and Schmidt, S. (2020) Artificial light-harvesting complexes enable Rieske oxygenase catalyzed hydroxylations in non-photosynthetic cells, *Angew. Chem. Int. Ed. 59*, 3982-3987.

[48] Lanfranchi, E., Trajkovic, M., Barta, K., de Vries, J. G., and Janssen, D. B. (2019) Exploring the selective demethylation of aryl methyl ethers with a *Pseudomonas* Rieske monooxygenase, *Chembiochem 20*, 118-125.
[49] Perry, C., de Los Santos, E. L. C., Alkhalaf, L. M., and Challis, G. L. (2018) Rieske non-heme iron-dependent oxygenases catalyse diverse reactions in natural product biosynthesis, *Nat. Prod. Rep. 35*, 622-632.
[50] Denisov, I. G., Makris, T. M., Sligar, S. G., and Schlichting, I. (2005) Structure and chemistry of cytochrome P450, *Chem. Rev. 105*, 2253-2277.
[51] Ortiz de Montellano, P. R. (2010) Hydrocarbon hydroxylation by cytochrome P450 enzymes, *Chem. Rev. 110*, 932-948.
[52] Green, J., and Dalton, H. (1989) Substrate specificity of soluble methane monooxygenase. Mechanistic implications, *J. Biol. Chem. 264*, 17698-17703.
[53] Wallar, B. J., and Lipscomb, J. D. (1996) Dioxygen activation by enzymes containing binuclear non-heme iron clusters, *Chem. Rev. 96*, 2625-2657.
[54] Liang, Y., Wei, J., Qiu, X., and Jiao, N. (2018) Homogeneous oxygenase catalysis, *Chem. Rev. 118*, 4912-4945.
[55] Hausinger, R. P. (2004) Fe(II)/alpha-ketoglutarate-dependent hydroxylases and related enzymes, *Crit. Rev. Biochem. Mol. Biol. 39*, 21-68.
[56] Kauppi, B., Lee, K., Carredano, E., Parales, R. E., Gibson, D. T., Eklund, H., and Ramaswamy, S. (1998) Structure of an aromatic-ring-hydroxylating dioxygenase-naphthalene 1,2-dioxygenase, *Structure 6*, 571-586.
[57] Batie, C. J., LaHaie, E., and Ballou, D. P. (1987) Purification and characterization of phthalate oxygenase and phthalate oxygenase reductase from *Pseudomonas cepacia*, *J. Biol. Chem. 262*, 1510-1518.
[58] Wolfe, M. D., Parales, J. V., Gibson, D. T., and Lipscomb, J. D. (2001) Single turnover chemistry and regulation of O_2 activation by the oxygenase component of naphthalene 1,2-dioxygenase, *J. Biol. Chem. 276*, 1945-1953.
[59] Hou, Y.-J., Guo, Y., Li, D.-F., and Zhou, N.-Y. (2021) Structural and biochemical analysis reveals a distinct catalytic site of salicylate 5-monooxygenase NagGH from Rieske dioxygenases, *Appl. Environ. Microbiol. 87*, e01629-20, doi:10.1128/aem.01629-20
[60] Dong, X., Fushinobu, S., Fukuda, E., Terada, T., Nakamura, S., Shimizu, K., Nojiri, H., Omori, T., Shoun, H., and Wakagi, T. (2005) Crystal structure of the terminal oxygenase component of cumene dioxygenase from *Pseudomonas fluorescens* IP01, *J. Bacteriol. 187*, 2483-2490.
[61] Friemann, R., Ivkovic-Jensen, M. M., Lessner, D. J., Yu, C.-L., Gibson, D. T., Parales, R. E., Eklund, H., and Ramaswamy, S. (2005) Structural insight into the dioxygenation of nitroarene compounds: The crystal structure of nitrobenzene dioxygenase, *J. Mol. Biol. 348*, 1139-1151.
[62] Kumari, A., Singh, D., Ramaswamy, S., and Ramanathan, G. (2017) Structural and functional studies of ferredoxin and oxygenase components of 3-nitrotoluene dioxygenase from *Diaphorobacter sp*. strain DS2, *PLoS One 12*, e0176398, doi:10.1371/journal.pone.0176398
[63] Jakoncic, J., Jouanneau, Y., Meyer, C., and Stojanoff, V. (2007) The catalytic pocket of the ring-hydroxylating dioxygenase from *Sphingomonas* CHY-1, *Biochem. Biophys. Res. Commun. 352*, 861-866.

[64] Furusawa, Y., Nagarajan, V., Tanokura, M., Masai, E., Fukuda, M., and Senda, T. (2004) Crystal structure of the terminal oxygenase component of biphenyl dioxygenase derived from *Rhodococcus sp*. strain RHA1, *J. Mol. Biol. 342*, 1041-1052.

[65] Kumar, P., Mohammadi, M., Viger, J.-F., Barriault, D., Gomez-Gil, L., Eltis, L. D., Bolin, J. T., and Sylvestre, M. (2011) Structural insight into the expanded PCB-degrading abilities of a biphenyl dioxygenase obtained by directed evolution, *J. Mol. Biol. 405*, 531-547.

[66] Friemann, R., Lee, K., Brown, E., N., Gibson, D., T., Eklund, H., and Ramaswamy, S. (2009) Structures of the multicomponent Rieske non-heme iron toluene 2,3-dioxygenase enzyme system, *Acta Crystallogr. Sect. D: Biol. Crystallogr. 65*, 24-33.

[67] Nojiri, H., Ashikawa, Y., Noguchi, H., Nam, J.-W., Urata, M., Fujimoto, Z., Uchimura, H., Terada, T., Nakamura, S., Shimizu, K., Yoshida, T., Habe, H., and Omori, T. (2005) Structure of the terminal oxygenase component of angular dioxygenase, carbazole 1,9a-dioxygenase, *J. Mol. Biol. 351*, 355-370.

[68] Martins, B. M., Svetlitchnaia, T., and Dobbek, H. (2005) 2-Oxoquinoline 8-monooxygenase oxygenase component: active site modulation by Rieske-[2Fe-2S] center oxidation/reduction, *Structure 13*, 817-824.

[69] Dumitru, R., Jiang, W. Z., Weeks, D. P., and Wilson, M. A. (2009) Crystal structure of dicamba monooxygenase: A Rieske nonheme oxygenase that catalyzes oxidative demethylation, *J. Mol. Biol. 392*, 498-510.

[70] Capyk, J. K., D'Angelo, I., Strynadka, N. C., and Eltis, L. D. (2009) Characterization of 3-ketosteroid 9α-hydroxylase, a Rieske oxygenase in the cholesterol degradation pathway of *Mycobacterium tuberculosis*, *J. Biol. Chem. 284*, 9937-9946.

[71] Daughtry, K. D., Xiao, Y., Stoner-Ma, D., Cho, E., Orville, A. M., Liu, P., and Allen, K. N. (2012) Quaternary ammonium oxidative demethylation: X-ray crystallographic, resonance Raman, and UV-visible spectroscopic analysis of a Rieske-type demethylase., *J. Am. Chem. Soc. 134*, 2823-2834.

[72] Lukowski, A. L., Liu, J., Bridwell-Rabb, J., and Narayan, A. R. H. (2020) Structural basis for divergent C-H hydroxylation selectivity in two Rieske oxygenases, *Nat. Commun. 11*, 2991, doi:10.1038/s41467-020-16729-0

[73] Erickson, E., Bleem, A., Kuatsjah, E., Werner, A. Z., DuBois, J. L., McGeehan, J. E., Eltis, L. D., and Beckham, G. T. (2022) Critical enzyme reactions in aromatic catabolism for microbial lignin conversion, *Nat. Catal. 5*, 86-98.

[74] Mahto, J. K., Neetu, N., Waghmode, B., Kuatsjah, E., Sharma, M., Sircar, D., Sharma, A. K., Tomar, S., Eltis, L. D., and Kumar, P. (2021) Molecular insights into substrate recognition and catalysis by phthalate dioxygenase from *Comamonas testosteroni*, *J. Biol. Chem. 297*, 101416, doi:10.1016/j.jbc.2021.101416

[75] Ferraro, D. J., Okerlund, A., Brown, E., and Ramaswamy, S. (2017) One enzyme, many reactions: structural basis for the various reactions catalyzed by naphthalene 1,2-dioxygenase, *IUCrJ 4*, 648-656.

[76] Parales, R. E., Lee, K., Resnick, S. M., Jiang, H., Lessner, D. J., and Gibson, D. T. (2000) Substrate specificity of naphthalene dioxygenase: effect of specific amino acids at the active site of the enzyme, *J. Bacteriol. 182*, 1641-1649.

[77] Liu, J., Tian, J., Perry, C., Lukowski, A. L., Doukov, T. I., Narayan, A. R. H., and Bridwell-Rabb, J. (2022) Design principles for site-selective hydroxylation by a Rieske oxygenase, *Nat. Commun. 13*, 255, doi:10.1038/s41467-021-27822-3

[78] Wolfe, M. D., Altier, D. J., Stubna, A., Popescu, C. V., Münck, E., and Lipscomb, J. D. (2002) Benzoate 1,2-dioxygenase from *Pseudomonas putida*: Single turnover kinetics and regulation of a two-component Rieske dioxygenase, *Biochemistry 41*, 9611-9626.

[79] Wolfe, M. D., and Lipscomb, J. D. (2003) Hydrogen peroxide-coupled *cis*-diol formation catalyzed by naphthalene 1,2-dioxygenase, *J. Biol. Chem. 278*, 829-835.

[80] Yang, T.-C., Wolfe, M. D., Neibergall, M. B., Mekmouche, Y., Lipscomb, J. D., and Hoffman, B. M. (2003) Substrate binding to NO-ferro-naphthalene 1,2-dioxygenase studied by high-resolution Q-band pulsed ^{2}H-ENDOR spectroscopy, *J. Am. Chem. Soc. 125*, 7056-7066.

[81] Pati, S. G., Bopp, C. E., Kohler, H.-P. E., and Hofstetter, T. B. (2022) Substrate-specific coupling of O_2 activation to hydroxylations of aromatic compounds by Rieske non-heme iron dioxygenases, *ACS Catal. 12*, 6444-6456.

[82] Sutherlin, K. D., Rivard, B. S., Bottger, L. H., Liu, L. V., Rogers, M. S., Srnec, M., Park, K., Yoda, Y., Kitao, S., Kobayashi, Y., Saito, M., Seto, M., Hu, M., Zhao, J., Lipscomb, J. D., and Solomon, E. I. (2018) NRVS studies of the peroxide shunt intermediate in a Rieske dioxygenase and its relation to the native Fe(II) O_2 reaction, *J. Am. Chem. Soc. 140*, 5544-5559.

[83] Bassan, A., Blomberg, M. R. A., Borowski, T., and Siegbahn, P. E. M. (2004) Oxygen activation by Rieske non-heme iron oxygenases, a theoretical insight, *J. Phys. Chem. B 108*, 13031-13041.

[84] Rivard, B. S., Rogers, M. S., Marell, D. J., Neibergall, M. B., Chakrabarty, S., Cramer, C. J., and Lipscomb, J. D. (2015) Rate-determining attack on substrate precedes Rieske cluster oxidation during *cis*-dihydroxylation by benzoate dioxygenase, *Biochemistry 54*, 4652-4664.

[85] Neibergall, M. B., Stubna, A., Mekmouche, Y., Münck, E., and Lipscomb, J. D. (2007) Hydrogen peroxide dependent *cis*-dihydroxylation of benzoate by fully oxidized benzoate 1,2-dioxygenase, *Biochemistry 46*, 8004-8016.

[86] Bugg, T. D. H., and Ramaswamy, S. (2008) Non-heme iron-dependent dioxygenases: unravelling catalytic mechanisms for complex enzymatic oxidations, *Curr. Opin. Chem. Biol. 12*, 134-140.

[87] Ohta, T., Chakrabarty, S., Lipscomb, J. D., and Solomon, E. I. (2008) Near-IR MCD of the nonheme ferrous active site in naphthalene 1,2-dioxygenase: Correlation to crystallography and structural insight into the mechanism of Rieske dioxygenases, *J. Am. Chem. Soc. 130*, 1601-1610.

[88] Guroff, G., Daly, J. W., Jerina, D. M., Renson, J., Witkop, B., and Udenfriend, S. (1967) Hydroxylation-induced migration: the NIH shift. Recent experiments reveal an unexpected and general result of enzymatic hydroxylation of aromatic compounds, *Science 157*, 1524-1530.

[89] Miller, R. J., and Benkovic, S. J. (1988) L-[2,5-H^2]phenylalanine, an alternate substrate for rat liver phenylalanine hydroxylase, *Biochemistry 27*, 3658-3663.

[90] Hillas, P. J., and Fitzpatrick, P. F. (1996) A mechanism for hydroxylation by tyrosine hydroxylase based on partitioning of substituted phenylalanines, *Biochemistry 35*, 6969-6975.

[91] Solomon, E. I., DeWeese, D. E., and Babicz, J. T. (2021) Mechanisms of O_2 activation by mononuclear non-heme iron enzymes, *Biochemistry 60*, 3497-3506.

[92] Gibson, D. T., Cardini, G. E., Maseles, F. C., and Kallio, R. E. (1970) Oxidative degradation of aromatic hydrocarbons by microorganisms. IV. Incorporation of oxygen-18 into benzene by *Pseudomonas putida*, *Biochemistry 9*, 1631-1635.
[93] Jeffrey, A. M., Yeh, H. J., Jerina, D. M., Patel, T. R., Davey, J. F., and Gibson, D. T. (1975) Initial reactions in the oxidation of naphthalene by *Pseudomonas putida*, *Biochemistry 14*, 575-584.
[94] Bassan, A., Blomberg, M. R. A., and Siegbahn, P. E. M. (2004) A theoretical study of the *cis*-dihydroxylation mechanism in naphthalene 1,2-dioxygenase, *J. Biol. Inorg. Chem. 9*, 439-452.
[95] Chakrabarty, S., Austin, R. N., Deng, D., Groves, J. T., and Lipscomb, J. D. (2007) Radical intermediates in monooxygenase reactions of Rieske dioxygenases, *J. Am. Chem. Soc. 129*, 3514-3515.
[96] Yoshida, H., Takeda, H., Wakana, D., Sato, F., and Hosoe, T. (2020) Identification of a multi-component berberine 11-hydroxylase from *Burkholderia sp*. strain CJ1, *Biosci. Biotechnol. Biochem. 84*, 1274-1284.
[97] Wackett, L. P., Kwart, L. D., and Gibson, D. T. (1988) Benzylic monooxygenation catalyzed by toluene dioxygenase from *Pseudomonas putida*, *Biochemistry 27*, 1360-1367.
[98] Li, P., Wang, L., and Feng, L. (2013) Characterization of a novel Rieske-type alkane monooxygenase system in *Pusillimonas* sp. strain T7-7, *J. Bacteriol. 195*, 1892-1901.
[99] Schäfer, F., Schuster, J., Würz, B., Härtig, C., Harms, H., Müller, R. H., and Rohwerder, T. (2012) Synthesis of short-chain diols and unsaturated alcohols from secondary alcohol substrates by the Rieske nonheme mononuclear iron oxygenase MdpJ., *Appl. Environ. Microbiol. 78*, 6280-6284.
[100] Lee, J., Simurdiak, M., and Zhao, H. (2005) Reconstitution and characterization of aminopyrrolnitrin oxygenase, a Rieske *N*-oxygenase that catalyzes unusual arylamine oxidation., *J. Biol. Chem. 280*, 36719-36727.
[101] Sydor, P. K., Barry, S. M., Odulate, O. M., Barona-Gomez, F., Haynes, S. W., Corre, C., Song, L., and Challis, G. L. (2011) Regio- and stereodivergent antibiotic oxidative carbocyclizations catalysed by Rieske oxygenase-like enzymes, *Nat. Chem. 3*, 388-392.
[102] Bernhardt, F. H., Pachowsky, H., and Staudinger, H. (1975) A 4-methoxybenzoate O-demethylase from *Pseudomonas putida.* A new type of monooxygenase system, *Eur. J. Biochem. 57*, 241-256.
[103] Summers, R. M., Louie, T. M., Yu, C. L., and Subramanian, M. (2011) Characterization of a broad-specificity non-haem iron N-demethylase from *Pseudomonas putida* CBB5 capable of utilizing several purine alkaloids as sole carbon and nitrogen source, *Microbiology-(UK) 157*, 583-592.
[104] Schmidt, S. (2022) Expanding the repertoire of Rieske oxygenases for O-demethylations, *Chem Catalysis 2*, 1843-1845.
[105] Bleem, A., Kuatsjah, E., Presley, G. N., Hinchen, D. J., Zahn, M., Garcia, D. C., Michener, W. E., König, G., Tornesakis, K., Allemann, M. N., Giannone, R. J., McGeehan, J. E., Beckham, G. T., and Michener, J. K. (2022) Discovery, characterization, and metabolic engineering of Rieske non-heme iron monooxygenases for guaiacol O-demethylation, *Chem Catalysis 2*, 1989-2011.
[106] Chartrain, M., Jackey, B., Taylor, C., Sandford, V., Gbewonyo, K., Lister, L., Dimichele, L., Hirsch, C., Heimbuch, B., Maxwell, C., Pascoe, D., Buckland, B., and Greasham, R.

(1998) Bioconversion of indene to cis (1S,2R) indandiol and trans (1R,2R) indandiol by *Rhodococcus* species, *J. Ferment. Bioeng. 86*, 550-558.

[107] Gibson, D. T., Resnick, S. M., Lee, K., Brand, J. M., Torok, D. S., Wackett, L. P., Schocken, M. J., and Haigler, B. E. (1995) Desaturation, dioxygenation, and monooxygenation reactions catalyzed by naphthalene dioxygenase from *Pseudomonas sp*. strain 9816-4, *J. Bacteriol. 177*, 2615-2621.

[108] Rogers, M. S., and Lipscomb, J. D. (2019) Salicylate 5-hydroxylase: intermediates in aromatic hydroxylation by a Rieske monooxygenase, *Biochemistry 58*, 5305-5319.

[109] Zhou, N.-Y., Al-Dulayymi, J., Baird, M. S., and Williams, P. A. (2002) Salicylate 5-hydroxylase from *Ralstonia* sp. strain U2: A monooxygenase with close relationships to and shared electron transport proteins with naphthalene dioxygenase, *J. Bacteriol. 184*, 1547-1555.

[110] Fuenmayor, S. L., Wild, M., Boyes, A. L., and Williams, P. A. (1998) A gene cluster encoding steps in conversion of naphthalene to gentisate in *Pseudomonas* sp. strain U2, *J. Bacteriol. 180*, 2522-2530.

[111] Fang, T., and Zhou, N.-Y. (2014) Purification and characterization of salicylate 5-hydroxylase, a three-component monooxygenase from *Ralstonia* sp. strain U2., *Appl. Microbiol. Biotechnol. 98*, 671-679.

[112] Guengerich, F. P. (2001) Common and uncommon cytochrome P450 reactions related to metabolism and chemical toxicity, *Chem. Res. Toxicol. 14*, 611-650.

[113] Podgorski, M. N., Coleman, T., Chao, R. R., De Voss, J. J., Bruning, J. B., and Bell, S. G. (2020) Investigation of the requirements for efficient and selective cytochrome P450 monooxygenase catalysis across different reactions, *J. Inorg. Biochem. 203*, 110913, doi:10.1016/j.jinorgbio.2019.110913

[114] Massey, V. (1994) Activation of molecular oxygen by flavins and flavoproteins, *J. Biol. Chem. 269*, 22459-22462.

[115] Hefti, M. H., Van Vugt-Van der Toorn, C. J. G., Dixon, R., and Vervoort, J. (2001) A novel purification method for histidine-tagged proteins containing a thrombin cleavage site, *Anal. Biochem. 295*, 180-185.

[116] Zhao, Y., and Truhlar, D. G. (2008) The M06 suite of density functionals for main group thermochemistry, thermochemical kinetics, noncovalent interactions, excited states, and transition elements: two new functionals and systematic testing of four M06-class functionals and 12 other functionals, *Theor. Chem. Acc. 120*, 215-241.

[117] Hehre, W. J., Random, L., Schleyer, P. v. R., and Pople, J. A. (1986) *Ab Initio Molecular Orbital Theory*, Wiley, New York.

[118] Frisch, M. J., Trucks, G. W., Schlegel, H. B., Scuseria, G. E., Robb, M. A., Cheeseman, J. R., Scalmani, G., Barone, V., Petersson, G. A., Nakatsuji, H., Li, X., Caricato, M., Marenich, A. V., Bloino, J., Janesko, B. G., Gomperts, R., Mennucci, B., Hratchian, H. P., Ortiz, J. V., Izmaylov, A. F., Sonnenberg, J. L., Williams, Ding, F., Lipparini, F., Egidi, F., Goings, J., Peng, B., Petrone, A., Henderson, T., Ranasinghe, D., Zakrzewski, V. G., Gao, J., Rega, N., Zheng, G., Liang, W., Hada, M., Ehara, M., Toyota, K., Fukuda, R., Hasegawa, J., Ishida, M., Nakajima, T., Honda, Y., Kitao, O., Nakai, H., Vreven, T., Throssell, K., Montgomery Jr, J. A., Peralta, J. E., Ogliaro, F., Bearpark, M. J., Heyd, J. J., Brothers, E. N., Kudin, K. N., Staroverov, V. N., Keith, T. A., Kobayashi, R., Normand, J., Raghavachari, K., Rendell, A. P., Burant, J. C., Iyengar, S. S., Tomasi, J., Cossi, M., Millam, J. M., Klene, M., Adamo, C., Cammi, R., Ochterski, J. W., Martin, R. L.,

Morokuma, K., Farkas, O., Foresman, J. B., and Fox, D. J. (2016) Gaussian 16 Rev. C.01, Wallingford, CT.
[119] Marenich, A. V., Cramer, C. J., and Truhlar, D. G. (2009) Universal solvation model based on solute electron density and on a continuum model of the solvent defined by the bulk dielectric constant and atomic surface tensions, *J. Phys. Chem. B 113*, 6378-6396.
[120] Marenich, A. V., Jerome, S. V., Cramer, C. J., and Truhlar, D. G. (2012) Charge model 5: An extension of Hirshfeld population analysis for the accurate description of molecular interactions in gaseous and condensed phases, *J. Chem. Theory Comput. 8*, 527-541.
[121] Chai, J.-D., and Head-Gordon, M. (2008) Long-range corrected hybrid density functionals with damped atom-atom dispersion corrections, *Phys. Chem. Chem. Phys. 10*, 6615-6620.
[122] Dennington, R., Keith, T. A., and Millam, J. M. (2016) GaussView 6.1, Semichem Inc., Shawnee Mission, Kansas.
[123] Tarasev, M., Rhames, F., and Ballou, D. P. (2004) Rates of the phthalate dioxygenase reaction with oxygen are dramatically increased by interactions with phthalate and phthalate oxygenase reductase, *Biochemistry 43*, 12799-12808.
[124] Beharry, Z. M., Eby, D. M., Coulter, E. D., Viswanathan, R., Neidle, E. L., Phillips, R. S., and Kurtz, D. M., Jr. (2003) Histidine ligand protonation and redox potential in the Rieske dioxygenases: Role of a conserved aspartate in anthranilate 1,2-dioxygenase, *Biochemistry 42*, 13625-13636.
[125] Brown, E. N., Friemann, R., Karlsson, A., Parales, J. V., Couture, M. M. J., Eltis, L. D., and Ramaswamy, S. (2008) Determining Rieske cluster reduction potentials, *J. Biol. Inorg. Chem. 13*, 1301-1313.
[126] Robertson, J. B., Spain, J. C., Haddock, J. D., and Gibson, D. T. (1992) Oxidation of nitrotoluenes by toluene dioxygenase: evidence for a monooxygenase reaction, *Appl. Environ. Microbiol. 58*, 2643-2648.
[127] Lee, K., and Gibson, D. T. (1996) Toluene and ethylbenzene oxidation by purified naphthalene dioxygenase from Pseudomonas sp. strain NCIB 9816-4, *Appl. Environ. Microbiol. 62*, 3101-3106.
[128] Pati, S. G., Kohler, H.-P. E., Bolotin, J., Parales, R. E., and Hofstetter, T. B. (2014) Isotope effects of enzymatic dioxygenation of nitrobenzene and 2-nitrotoluene by nitrobenzene dioxygenase, *Environ. Sci. Technol. 48*, 10750-10759.
[129] Yang, T.-C., Wolfe, M. D., Neibergall, M. B., Mekmouche, Y., Lipscomb, J. D., and Hoffman, B. M. (2003) Modulation of substrate binding to naphthalene 1,2-dioxygenase by Rieske cluster reduction/oxidation, *J. Am. Chem. Soc. 125*, 2034-2035.
[130] Ashikawa, Y., Fujimoto, Z., Usami, Y., Inoue, K., Noguchi, H., Yamane, H., and Nojiri, H. (2012) Structural insight into the substrate- and dioxygen-binding manner in the catalytic cycle of Rieske nonheme iron oxygenase system, carbazole 1,9a-dioxygenase, *BMC Struct. Biol. 12*, 15, doi:10.1186/1472-6807-12-15
[131] Boyd, D. R., Daly, J. W., and Jerina, D. M. (1972) Rearrangement of [1-^{2}H]- and [2-^{2}H]naphthalene 1,2-oxides to 1-naphthol. Mechanism of the NIH shift, *Biochemistry 11*, 1961-1966.
[132] Vannelli, T., and Hooper, A. B. (1995) NIH shift in the hydroxylation of aromatic compounds by the ammonia-oxidizing bacterium *Nitrosomonas europaea*. Evidence against an arene oxide intermediate, *Biochemistry 34*, 11743-11749.
[133] Dear, G. J., Ismail, I. M., Mutch, P. J., Plumb, R. S., Davies, L. H., and Sweatman, B. C. (2000) Urinary metabolites of a novel quinoxaline non-nucleoside reverse transcriptase

inhibitor in rabbit, mouse and human: identification of fluorine NIH shift metabolites using NMR and tandem MS, *Xenobiotica 30*, 407-426.
[134] Koerts, J., Soffers, A. E., Vervoort, J., De Jager, A., and Rietjens, I. M. (1998) Occurrence of the NIH shift upon the cytochrome P450-catalyzed in vivo and in vitro aromatic ring hydroxylation of fluorobenzenes, *Chem Res Toxicol 11*, 503-512.
[135] Wackett, L. P. (2021) Why Is the biodegradation of polyfluorinated compounds so rare?, *mSphere 6*, e0072121, doi:10.1128/mSphere.00721-21
[136] Wang, Y., and Liu, A. (2020) Carbon-fluorine bond cleavage mediated by metalloenzymes, *Chem. Soc. Rev. 49*, 4906-4925.
[137] Wang, Y., Davis, I., Shin, I., Xu, H., and Liu, A. (2021) Molecular rationale for partitioning between C–H and C–F bond activation in heme-dependent tyrosine hydroxylase, *J. Am. Chem. Soc. 143*, 4680-4693.
[138] Engesser, K. H., Schmidt, E., and Knackmuss, H. J. (1980) Adaptation of *Alcaligenes eutrophus* B9 and *Pseudomonas sp.* B13 to 2-fluorobenzoate as growth substrate, *Appl. Environ. Microbiol. 39*, 68-73.
[139] Tong, W., Huang, Q., Li, M., and Wang, J.-b. (2019) Enzyme-catalyzed C–F bond formation and cleavage, *Bioresour. Bioprocess. 6*, 46, doi:10.1186/s40643-019-0280-6
[140] Hidde Boersma, F. G., Colin McRoberts, W., Cobb, S. L., and Murphy, C. D. (2004) A ^{19}F NMR study of fluorobenzoate biodegradation by *Sphingomonas sp.* HB-1, *FEMS Microbiol. Lett. 237*, 355-361.
[141] Münch, J., Püllmann, P., Zhang, W., and Weissenborn, M. J. (2021) Enzymatic hydroxylations of sp^3-carbons, *ACS Catal. 11*, 9168-9203.
[142] Griffin, G. W., and Horn, K. A. (1987) Kinetic isotope effects as probes of the mechanism of reaction of 1-naphthylcarbene with cyclohexane and toluene, *J. Am. Chem. Soc. 109*, 4919-4926.
[143] Zhu, L., Zhou, J., Zhang, R., Tang, X., Wang, J., Li, Y., Zhang, Q., and Wang, W. (2020) Degradation mechanism of biphenyl and 4-4'-dichlorobiphenyl cis-dihydroxylation by non-heme 2,3 dioxygenases BphA: A QM/MM approach, *Chemosphere 247*, doi:10.1016/j.chemosphere.2020.125844
[144] Hanzlik, R. P., Schaefer, A. R., Moon, J. B., and Judson, C. M. (1987) Primary and secondary kinetic deuterium isotope effects and transition-state structures for benzylic chlorination and bromination of toluene, *J. Am. Chem. Soc. 109*, 4926-4930.
[145] Gray, H. B., and Winkler, J. R. (1996) Electron transfer in proteins, *Ann. Rev. Biochem. 65*, 537-561.
[146] Priestley, N. D., Floss, H. G., Froland, W. A., Lipscomb, J. D., Williams, P. G., and Morimoto, H. (1992) Cryptic stereospecificity of methane monooxygenase, *J. Am. Chem. Soc. 114*, 7561-7562.
[147] Austin, R. N., Chang, H.-K., Zylstra, G. J., and Groves, J. T. (2000) The non-heme diiron alkane monooxygenase of *Pseudomonas oleovorans* (AlkB) hydroxylates via a substrate radical intermediate, *J. Am. Chem. Soc. 122*, 11747-11748.
[148] Martinie, R. J., Livada, J., Chang, W.-c., Green, M. T., Krebs, C., Bollinger, J. M., and Silakov, A. (2015) Experimental correlation of substrate position with reaction outcome in the aliphatic halogenase, SyrB2, *J. Am. Chem. Soc. 137*, 6912-6919.
[149] Groves, J. T. (2003) The bioinorganic chemistry of iron in oxygenases and supramolecular assemblies, *Proc. Natl. Acad. Sci. U. S. A.. 100*, 3569-3574.

[150] Banerjee, R., Jones, J. C., and Lipscomb, J. D. (2019) Soluble methane monooxygenase, *Ann. Rev. Biochem. 88*, 409-431.
[151] Tian, G., and Klinman, J. P. (1993) Discrimination between ^{16}O and ^{18}O in oxygen binding to the reversible oxygen carriers hemoglobin, myoglobin, hemerythrin, and hemocyanin: a new probe for oxygen binding and reductive activation by proteins, *J. Am. Chem. Soc. 115*, 8891-8897.
[152] Roth, J. P., and Klinman, J. P. (2006) Oxygen-18 isotope effects as a probe of enzymatic activation of molecular oxygen, In *Isotope Effects in Chemistry and Biology* (Limbach, H. H., and Kohen, A., Eds.), pp 645-669, CRC Press, Alden Books, London.
[153] Mirica, L. M., McCusker, K. P., Munos, J. W., Liu, H.-w., and Klinman, J. P. (2008) ^{18}O kinetic isotope effects in non-heme iron enzymes: probing the nature of Fe/O_2 intermediates, *J. Am. Chem. Soc. 130*, 8122-8123.
[154] Karlsson, A., Parales, J. V., Parales, R. E., Gibson, D. T., Eklund, H., and Ramaswamy, S. (2003) Crystal structure of naphthalene dioxygenase: Side-on binding of dioxygen to iron, *Science 299*, 1039-1042.
[155] Cleland, W. W. (1975) What limits the rate of an enzyme-catalyzed reaction?, *Acc. Chem. Res. 8*, 145-151.
[156] Lehnert, N., Ho, R. Y. N., Que, L., Jr., and Solomon, E. I. (2001) Spectroscopic properties and electronic structure of low-spin Fe(III)-alkylperoxo complexes: Homolytic cleavage of the O-O bond, *J. Am. Chem. Soc. 123*, 8271-8290.
[157] Lehnert, N., Fujisawa, K., and Solomon, E. I. (2003) Electronic structure and reactivity of high-spin iron-alkyl- and -pterinperoxo complexes, *Inorg. Chem. 42*, 469-481.

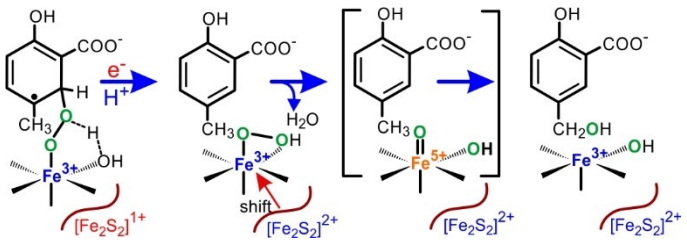

For Table of Contents use only